Probability Distribution of the Maximum Response of Structures Subjected to Nonstationary Random Earthquake Motion

By

Hiroyuki KAMEDA*

(Received June 28, 1971)

Presented are the results of a theoretical analysis of the statistical properties of the maximum structural response to nonstationary random earthquake motion. Two approximate methods were developed to obtain the probability distribution of the maximum earthquake response on the basis of the pure-birth process equation and the peak envelope distribution, which should be adopted alternatively depending on the range of the structural and excitation parameters. Also discussed is a concept of structural design for random earthquake loads on the basis of the numerical results.

1. Introductien

When civil engineering structures are subjected to random excitations of the earthquake type, their dynamic responses obviously fluctuate in a random manner as well. Similar cases occur when wind forces which are distributed randomly either in time or space act upon flexible structures or when random pulses of vehicular loads move along bridge girders.

In discussing the strength of structures in withstanding such random loads, we are primarily interested in the probability of structural safety during the service life, which is referred to as the reliability function defined[4] by

$$R_f(T)=\int_0^\infty \Phi_f(Y,T)f_s(Y,T)dY$$

where $\Phi_f(Y,T)$ denotes the probability that the structural "response level" will not exceed Y in the future interval T, and $f_s(Y,T)$ is the probability density of the "strength" Y of the structure.

If we neglect the effect of the random distribution of the strength of structures about its mean value Y_s and set

$$f_s(Y,T)=\delta(Y-Y_s)$$

* Department of Transportation Engineering

then we have

$$R_f(T)=\int_0^\infty \Phi_f(Y,T)\delta(Y-Y_s)dY=\Phi_f(Y_s,T)$$

which implies that the reliability is directly given by the probability that the "response level" will not exceed the mean strength Y_s throughout the period T.

It is frequently the cases in design practice that structural safety is stipulated as the requirement that the maximum response given either in terms of stress, deflection, or displacement be not in excess of the prescribed allowable value, in which case $\Phi_f(Y,T)$ coincides with the probability distribution of the maximum response, the main subject of this paper.

Compared with the instantaneous probabilistic properties of the random structural response, the theoretical discussion of the maximum response of a structure in some finite duration of continuous excitation poses a very difficult problem due to the vibrational characteristics of structures; this seems to have limited the appearance of very many successful papers in this field.

E. Rosenblueth and J. I. Bustamante[17] analyzed the "response" r, which is approximately proportional to the square root of the sum of the kinetic energy and the strain energy of a simple structure subjected to a white-noise excitation, and obtained the probability distribution of its maximum value in the transient state with the aid of a diffusion process analogy; this was followed by a discussion in relation to the earthquake-resistant design of structures. As far as the author knows, this work was the first successful attempt to obtain a theoretical expression for the probability distribution of the maximum structural response to earthquakes. It is, however, confined to a white-noise excitation which cannot take account of the nonstationarity in amplitude and non-white spectral characteristics of general earthquake ground motions.

A. M. Freudenthal and M. Shinozuka[3] derived formulae for the upper and lower bounds of the probability distribution of the maximum structural response to an arbitrary random excitation of the earthquake type. However, the results of the application of their method to structures with a single degree of freedom show that the upper and lower bounds thus obtained are sometimes apart by one or two decimal points[18] which could not be said to be close enough for engineering application.

A. G. Davenport[2] and S. Komatsu[15] discussed the probability distribution of the maximum response of structures under wind loadings. Their methods of analysis differed in the concept of the time dependence of the mean intensity of the wind load, but they both assume that the statistical properties of the

response at a certain instant are independent of its past history. This means that the process of the upward or downward crossing of a certain response level becomes a Poisson process if the response is stationary. Y. Yamada and H. Takemiya[20] derived the non-excess probability of the maximum structural response to random earthquake motions under the same assumption. This assumption was also used by the author[6~8] and has proved appropriate in the analysis of earthquake ground motion, which contains a relatively wide range of frequency components.

On the contrary, this assumption fails to be accurate in the discussion of the random vibration of structures. The difficulty arises from the fact that many civil engineering structures exhibit relatively low dynamic damping, say 1~20 percent of critical damping. When such structures are subjected to random excitation, their response behaves as a continuous narrow-band random process which implies a high correlation between the response amplitudes at different times. Hence, the simple assumption of the history-independence of response, the Poisson process approximation in the case of a stationary response, needs to be examined as to its accuracy.

Thus, there are some basic problems left to be solved with regard to the theoretical representation of the probability distribution of the maximum response. In this study, two methods of analysis have been developed to furnish better approximate solutions; one, by taking due consideration of the above-mentioned correlation of responses at different times in solving the pure-birth-process equation, and the other, by applying the technique of the peak envelope distribution. It has been proved on the basis of the results of numerical surveys that these two methods can be applied alternatively to cover a wide range of parameters of practical interest.

2. Representation of Random Earthquake Acceleration

When we discuss the maximum ground motion in a strog earthquake, it suffices to treat the ground motion as a stationary random process[6~8]. However, when the structural response is in question, its transient part must be considered in the analysis since the effect of the initial conditions on the response is appreciable. Hence, in this section we shall introduce a statistical model of nonstationary earthquake motion to be used in the subsequent analysis.

The ground acceleration $\ddot{z}(t)$ in earthquakes shall be expressed in the form[6~8]

$$\ddot{z}(t)=\beta f(t;\tau)g(t) \qquad \cdots\cdots\cdots(1)$$

where $g(t)$ is a stationary random process with zero mean value, the variance of unity and the power spectrum $S_g(\omega)$, $f(t;\tau)$ is a deterministic shape function which exclusively assumes positive values, and β is a constant with the dimension of acceleration.

The appropriateness of representing the ground acceleration by the form of Eq. (1) was discussed by K. Toki[19] in connection with its spectral characteristics and was admitted for some typical strong motion accelerograph records. The shape function $f(t;\tau)$ may take any form, varying with the location of the observation site relative to the hypocenter, the characteristics of the seismic pulses generated at the origin, the path characteristics, the observation site conditions, etc. In the present study, an expression with a linear initial set up and an exponential subsiding tail[3] shall be adopted; i.e.,

$$f(t;\tau)=\frac{(1+\xi)^{(1+1/\xi)}}{\xi}e^{-st}(1-e^{-\xi st}) \qquad \cdots\cdots\cdots(2)$$

where s and ξ are the parameters determining the shape of $f(t;\tau)$. This $f(t;\tau)$ assumes the maximum value of unity at

$$t=t_m=\frac{1}{s\xi}\log(1+\xi)$$

Fig. 1 shows the shape function $f(t;\tau)$ of this type, and the values of ξ for various st_m are tabulated in Table 1. The variances and the correlation coefficient related to $\dot{z}(t)$ thus defined and the probability distribution $\Phi_s(\alpha)$ of the maximum ground acceleration can be discussed in the same manner as in the earlier studies[6~8], from which the expected value $\mathrm{E}[\alpha]$ of the maximum ground acceleration α is calculated (see Appendix) from

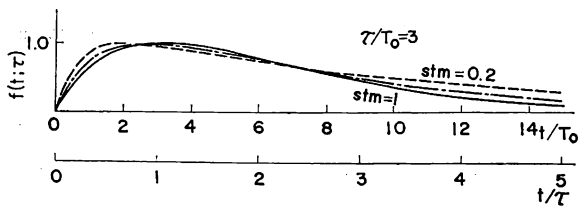

Fig. 1. Shape Function $f(t;\tau)$ of Earthquake Motion.

$$\mathrm{E}[\alpha]=\int_0^\infty\{1-\Phi_s(\alpha)\}d\alpha \qquad \cdots\cdots\cdots(3)$$

The duration of the ground motion for the present type of $f(t;\tau)$ cannot be defined explicitly since the exponential tail vanishes only in the limit of $t\to\infty$. Hence the "equivalent duration" τ shall be defined as the duration of a portion of a stationary ground motion $\beta g(t)$ whose expected value $\mathrm{E}[\alpha]$ of

the maximum ground acceleration is equal to that of the nonstationary ground motion in the present discussion. Hence if the power spectrum $S_g(\omega)$ of $g(t)$ is specified, we can determine the relationships between the equivalent duration τ, the mean maximum ground acceleration $E[\alpha]$, and the parameters s and ξ in Eq. (2). This procedure is illustrated in Fig. 2 for the case where the power spectrum $S_g(\omega)$ takes the form adopted in references 6)~8) and $g(t)$ is a Gaussian stationary process. The $s/\omega_0-E[\alpha]/\beta$ relationship in quadrant (a) of the figure has been obtained by applying the present model of the ground motion. On the other hand, the $E[\alpha]/\beta-\tau/T_0$ curve in quadrant (b) can readily be drawn from the results of the studies in references 6)~8) in which the stationary model of the ground motion has been adopted. Then the $s/\omega_0-\tau/T_0$ relation is obtained as in quadrant (c) by following the route shown by the dotted line. The $s/\omega_0-\tau/T_0$ curves thus obtained and plotted in logarithmic scales are nearly straight lines. The result in Fig. 2(c) would allow us to express it as

$$\frac{s}{\omega_0}=C\left(\frac{\tau}{T_0}\right)^{-1.09} \qquad \cdots\cdots\cdots(4)$$

The numerical values assigned to the coefficient C are indicated in Table 1. The τ/T_0 scale in Fig. 2 has been determined in such a manner.

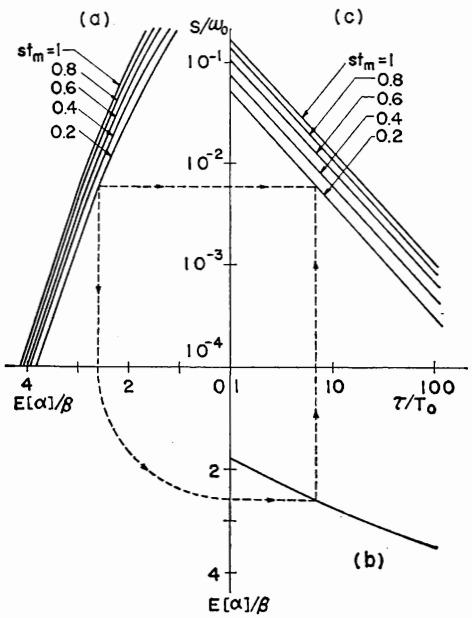

Fig. 2. Determination of the Equivalent Duration of Earthquake Motion.

Table 1. Parameters to Characterize the Shape Function.

st_m	ξ	C
1.0	0.0	0.166
0.8	0.539	0.136
0.6	1.579	0.108
0.4	4.047	0.077
0.2	13.30	0.050

In the analysis of structural response in subsequent subsections, it is desirable that the hight of the peak of the power spectrum $S_g(\omega)$ be chosen arbitrarily according to an independent parameter. Hence, in the sequel, $S_g(\omega)$ shall be represented in the following form analogous to the power spectrum of the relative velocity response of a simple structure subjected to white-noise excitation:

$$S_g(\omega)=\frac{4h_0}{\pi\omega_0}\frac{(\omega/\omega_0)^2}{\{1-(\omega/\omega_0)^2\}^2+4h_0^2(\omega/\omega_0)^2} \quad \cdots\cdots(5)$$

in which ω_0 is the predominant circular frequency. In the above structural analogy, h_0 corresponds to the damping factor. However, it does not necessarily stand for the damping factor of the ground of the observation site, but should be understood as a general parameter inclusive of other factors which would affect the peak value $S_g(\omega_0)$ given by

$$S_g(\omega_0)=\frac{1}{\pi h_0\omega_0} \quad \cdots\cdots(6)$$

It is readily verified that Eq. (5) satisfies the condition that $g(t)$ should have the variance of unity:

$$\int_0^\infty S_g(\omega)d\omega=1$$

It is expected that there would need to be some modification of Fig. 2 when $S_g(\omega)$ of the form of Eq. (5) is used with various values of h_0. Nevertheless, for simplicity, we shall use this figure to relate the equivalent duration τ of the nonstationary earthquake excitation to its relevant parameters.

3. Variances and Correlation Coefficients of Structural Response

(1) Simple Structure Considered

Throughout this study, we shall deal exclusively with a simple structure which can be represented by linear oscillator with a single degree of freedom. The equation of motion for such a system subjected to a ground acceleration $\ddot{z}(t)$ is given by

$$\ddot{y}(t)+2h_n\omega_n\dot{y}(t)+\omega_n^2y(t)=-\ddot{z}(t) \quad \cdots\cdots(7)$$

where $y(t)$: relative displacement, $\omega_n=\sqrt{k/m}$: natural circular frequency, $h_n=c/2\sqrt{mk}$: fraction of critical damping (damping factor), and m, k, and c: mass, spring constant, and damping coefficient of the system, respectively.

The solution of Eq. (7) under the initial conditions $y(0)=0$ and $\dot{y}(0)=0$ is represented by the well known convolution integral:

$$y(t)=-\frac{1}{\omega_n}\int_0^t h(t-\tau')\ddot{z}(\tau')d\tau' \qquad \cdots\cdots(8)$$

in which

$$h(t)=e^{-h_n\omega_n t}\sin\bar{\omega}_n t,\quad \bar{\omega}_n=\sqrt{1-h_n^2}\,\omega_n$$

Likewise, the velocity response $\dot{y}(t)$ is obtained as

$$\dot{y}(t)=-\frac{1}{\bar{\omega}_n}\int_0^t \dot{h}(t-\tau')\ddot{z}(\tau')d\tau' \qquad \cdots\cdots(9)$$

where

$$\dot{h}(t)=\bar{\omega}_n e^{-h_n\omega_n t}(\cos\bar{\omega}_n t-\bar{h}_n\sin\bar{\omega}_n t)$$

$$\bar{h}_n=h_n/\sqrt{1-h_n^2}$$

(2) Variances and Correlation Coefficients of Response

When the excitation $\ddot{z}(t)$ in Eq. (7) is a random process with zero mean value, the variances $\sigma_y^2(t)$, $\sigma_{\dot{y}}^2(t)$ of $y(t)$, $\dot{y}(t)$ are given, respectively, by

$$\left.\begin{aligned}\sigma_y^2(t)&=\mathrm{E}[y^2(t)]=\frac{1}{\bar{\omega}_n^2}\int_0^t h(t-t')dt'\int_0^t h(t-t'')\mathrm{E}(\ddot{z}(t')\ddot{z}(t''))]dt''\\ \text{and}\\ \sigma_{\dot{y}}^2(t)&=\mathrm{E}[\dot{y}^2(t)]=\frac{1}{\bar{\omega}_n^2}\int_0^t \dot{h}(t-t')dt'\int_0^t \dot{h}(t-t'')\mathrm{E}[\ddot{z}(t')\ddot{z}(t'')]dt''\end{aligned}\right\}\cdots\cdots(10)$$

In the same manner, the correlation coefficients $\rho_{y\dot{y}}(t)$ between $y(t)$ and $\dot{y}(t)$, $\rho_{yy}(t_1,t_2)$ between $y(t_1)$ and $y(t_2)$, and $\rho_{y\dot{y}}(t_1,t_2)$ between $y(t_1)$ and $\dot{y}(t_2)$ are represented, respectively, in the form

$$\left.\begin{aligned}\rho_{y\dot{y}}(t)&=\mathrm{E}[y(t)\dot{y}(t)]/\{\sigma_y(t)\sigma_{\dot{y}}(t)\}\\ &=\frac{1}{\sigma_y(t)\sigma_{\dot{y}}(t)\bar{\omega}_n^2}\int_0^t h(t-t')dt'\int_0^t \dot{h}(t-t'')\mathrm{E}[\ddot{z}(t')\ddot{z}(t'')]dt''\\ \rho_{yy}(t_1,t_2)&=\mathrm{E}[y(t_1)y(t_2)]/\{\sigma_y(t_1)\sigma_y(t_2)\}\\ &=\frac{1}{\sigma_y(t_1)\sigma_y(t_2)\bar{\omega}_n^2}\int_0^{t_1} h(t_1-t')dt'\int_0^{t_2} h(t_2-t'')\mathrm{E}[\ddot{z}(t')\ddot{z}(t'')]dt''\\ \rho_{y\dot{y}}(t_1,t_2)&=\mathrm{E}[y(t_1)\dot{y}(t_2)]/\{\sigma_y(t_1)\sigma_{\dot{y}}(t_2)\}\\ &=\frac{1}{\sigma_y(t_1)\sigma_{\dot{y}}(t_2)\bar{\omega}_n^2}\int_0^{t_1} h(t_1-t')dt'\int_0^{t_2} \dot{h}(t_2-t'')\mathrm{E}[\ddot{z}(t')\ddot{z}(t'')]dt''\end{aligned}\right\}\cdots(11)$$

When $\ddot{z}(t)$ takes the form of Eq. (1), we have

$$\begin{aligned}\mathrm{E}[\ddot{z}(t')\ddot{z}(t'')]&=\beta^2 f(t';\tau)f(t'';\tau)\mathrm{E}[g(t')g(t'')]\\ &=\beta^2 f(t';\tau)f(t'';\tau)\int_0^\infty S_g(\omega)\cos\omega(t'-t'')d\omega\end{aligned}\qquad\cdots\cdots(12)$$

On substitution in Eqs. (10) and (11) from Eqs. (2), (8), (9), and (12), and after an analytical procedure of integration with respect to time, we obtain the variances and the correlation coefficients of the nonstationary response in

the form of integrals with respect to the frequency.[13,14] If we make an approximate evaluation of these integrals by means of the method of T. K. Caughey and H. J. Stumpf[1], then some cumbersome algebra of contour integration leads to the following approximate formulae:

$$\left.\begin{aligned}\sigma_y^2(t) &\cong \frac{\pi\beta^2A^2}{\omega_n^3\zeta^2}S_g(\omega_n)K_{o1}(t,s,\xi)\\ \sigma_{\dot y}^2(t) &\cong \frac{\pi\beta^2A^2}{\omega_n}S_g(\omega_n)\{K_{o2}(t,s,\xi)-2\bar h_nK_{o3}(t,s,\xi)+\bar h_n^2K_{o1}(t,s,\xi)\}\end{aligned}\right\}\cdots(13)$$

$$\left.\begin{aligned}\rho_{y\dot y}(t) &\cong \frac{\pi\beta^2A^2S_g(\omega_n)}{\omega_n^2\zeta\sigma_y(t)\sigma_{\dot y}(t)}\{K_{o3}(t,s,\xi)-\bar h_nK_{o1}(t,s,\xi)\}\\ \rho_{yy}(t_1,t_2) &\cong \frac{\pi\beta^2A^2S_g(\omega_n)}{\omega_n^3\zeta^2\sigma_y(t_1)\sigma_y(t_2)}\{K_{c1}(t_1,t_2,s,\xi)+K_{s4}(t_1,t_2,s,\xi)\}\\ \rho_{y\dot y}(t_1,t_2) &\cong \frac{\pi\beta^2A^2S_g(\omega_n)}{\omega_n^2\zeta\sigma_y(t_y)\sigma_{\dot y}(t_2)}[K_{c3}(t_1,t_2,s,\xi)+K_{s5}(t_1,t_2,s,\xi)\\ &\qquad -\bar h_n\{K_{c1}(t_1,t_2,s,\xi)+K_{s4}(t_1,t_2,s,\xi)\}]\end{aligned}\right\}\cdots\cdots(14)$$

where

$$K_{oi}(t,s,\xi)=L_{oi}(t,s)+L_{oi}(t,(1+\xi)s)-U_{oi}(t,s,(1+\xi)s)-U_{oi}(t,(1+\xi)s,s)\,;\quad(i=1,2,3)$$

in which

$$L_{o1}(t,s)=\frac{\zeta^2}{4\lambda(s)(\zeta^2+\lambda^2(s))}\left\{e^{-2st}-e^{-2h_n\omega_nt}\left(1+\frac{\lambda(s)}{\zeta}\sin 2\bar\omega_nt+2\frac{\lambda^2(s)}{\zeta^2}\sin^2\bar\omega_nt\right)\right\}$$

$$L_{o2}(t,s)=\frac{\zeta^2}{4\lambda(s)(\zeta^2+\lambda^2(s))}\left\{\left(1+2\frac{\lambda^2(s)}{\zeta^2}\right)e^{-2st}-e^{-2h_n\omega_nt}\cdot\left(1-\frac{\lambda(s)}{\zeta}\sin 2\bar\omega_nt+2\frac{\lambda^2(s)}{\zeta^2}\cos^2\bar\omega_nt\right)\right\}$$

$$L_{o3}(t,s)=\frac{\zeta}{4(\zeta^2+\lambda^2(s))}\left\{e^{-2st}-e^{-2h_n\omega_nt}\left(\cos 2\bar\omega_nt+\frac{\lambda(s)}{\zeta}\sin 2\bar\omega_nt\right)\right\}$$

$$U_{o1}(t,s,s')=\frac{\zeta^2}{2(\lambda(s)+\lambda(s'))(\zeta^2+\lambda^2(s))}[2\mu_1(s,s')e^{-(s+s')t}-e^{-2h_n\omega_nt}\{2\mu_1(s,s')\cos^2\bar\omega_nt+2\mu_2(s,s')\sin^2\bar\omega_nt-(\mu_3(s,s')-\mu_4(s,s'))\sin 2\bar\omega_nt\}]$$

$$U_{o2}(t,s,s')=\frac{\zeta^2}{2(\lambda(s)+\lambda(s'))(\zeta^2+\lambda^2(s))}[2\mu_2(s,s')e^{-(s+s')t}-e^{-2h_n\omega_nt}\{2\mu_2(s,s')\cos^2\bar\omega_nt+2\mu_1(s,s')\sin^2\bar\omega_nt+(\mu_3(s,s')-\mu_4(s,s'))\sin 2\bar\omega_nt\}]$$

$$U_{o3}(t,s,s')=\frac{-\zeta^2}{2(\lambda(s)+\lambda(s'))(\zeta^2+\lambda^2(s))}[(\mu_3(s,s')$$

$$-\mu_4(s, s'))e^{-(s+s')t}-e^{-2h_n\omega_n t}\{(\mu_3(s, s')$$
$$-\mu_4(s, s'))\cos 2\bar{\omega}_n t+(\mu_1(s, s')-\mu_2(s, s'))\sin 2\bar{\omega}_n t\}]$$

and

$$K_{ci}(t_1, t_2, s, \xi)=L_{ci}(t_1, t_2, s)+L_{ci}(t_1, t_2, (1+\xi)s)$$
$$-U_{ci}(t_1, t_2, s, (1+\xi)s)-U_{ci}(t_1, t_2, (1+\xi)s, s)\ ;\quad (i=1, 3)$$
$$K_{si}(t_1, t_2, s, \xi)=L_{si}(t_1, t_2, s)+L_{si}(t_1, t_2, (1+\xi)s)$$
$$-U_{si}(t_1, t_2, s, (1+\xi)s)-U_{si}(t_1, t_2, (1+\xi)s, s)\ ;\quad (i=4, 5)$$

in which

$$L_{c1}(t_1, t_2, s)|_{2t_1-t_2\geq 0}=\frac{\zeta^2}{4\lambda(s)(\zeta^2+\lambda^2(s))}\Big\{e^{-(2st_1+h_n\omega_n(t_2-t_1))}$$
$$\cdot\Big\{\cos\bar{\omega}_n(t_2-t_1)+\frac{\lambda(s)}{\zeta}\sin\bar{\omega}_n(t_2-t_1)\Big\}+\frac{1}{2}e^{-h_n\omega_n(t_2+t_1)}$$
$$\cdot\Big\{\cos\bar{\omega}_n(t_2-t_1)+\frac{\lambda(s)}{\zeta}\sin\bar{\omega}_n(t_2+t_1)+2\frac{\lambda^2(s)}{\zeta^2}\sin\bar{\omega}_n t_2\sin\bar{\omega}_n t_1\Big\}$$
$$-\frac{1}{2}e^{-(h_n\omega_n(t_2+t_1)-2\lambda(s)\omega_n(t_2-t_1))}\Big\{\cos\bar{\omega}_n(t_2-t_1)$$
$$+\frac{\lambda(s)}{\zeta}\sin\bar{\omega}_n(3t_1-t_2)+2\frac{\lambda^2(s)}{\zeta^2}\sin\bar{\omega}_n t_1\sin\bar{\omega}_n(2t_1-t_2)\Big\}\Big\}$$

$$L_{c3}(t_1, t_2, s)|_{2t_1-t_2\geq 0}=\frac{\zeta^2}{4\lambda(s)(\zeta^2+\lambda^2(s))}\Big\{e^{-(2st_1+h_n\omega_n(t_2-t_1))}$$
$$\cdot\Big\{\frac{\lambda(s)}{\zeta}\cos\bar{\omega}_n(t_2-t_1)+\frac{\lambda^2(s)}{\zeta^2}\sin\bar{\omega}_n(t_2-t_1)\Big\}+\frac{1}{2}e^{-h_n\omega_n(t_2+t_1)}$$
$$\cdot\Big\{\sin\bar{\omega}_n(t_2-t_1)-\frac{\lambda(s)}{\zeta}\cos\bar{\omega}_n(t_2+t_1)-2\frac{\lambda^2(s)}{\zeta^2}\cos\bar{\omega}_n t_2\sin\bar{\omega}_n t_1\Big\}$$
$$-\frac{1}{2}e^{-(h_n\omega_n(t_2+t_1)-2\lambda(s)\omega_n(t_2-t_1))}\Big\{\sin\bar{\omega}_n(t_2-t_1)$$
$$+\frac{\lambda(s)}{\zeta}\cos\bar{\omega}_n(3t_1-t_2)+2\frac{\lambda^2(s)}{\zeta^2}\sin\bar{\omega}_n t_1\cos\bar{\omega}_n(2t_1-t_2)\Big\}\Big\}$$

$$L_{s4}(t_1, t_2, s)|_{2t_1-t_2\geq 0}=\frac{-\zeta^2}{8\lambda(s)(\zeta^2+\lambda^2(s))}\Big\{e^{-h_n\omega_n(t_2+t_1)}$$
$$\cdot\Big\{\cos\bar{\omega}_n(t_2-t_1)+\frac{\lambda(s)}{\zeta}\sin\bar{\omega}_n(t_2+t_1)+2\frac{\lambda^2(s)}{\zeta^2}\sin\bar{\omega}_n t_2\sin\bar{\omega}_n t_1\Big\}$$
$$-e^{-(h_n\omega_n(t_2+t_1)-2\lambda(s)\omega_n(t_2-t_1))}\Big\{\cos\bar{\omega}_n(t_2-t_1)$$
$$+\frac{\lambda(s)}{\zeta}\sin\bar{\omega}_n(3t_1-t_2)+2\frac{\lambda^2(s)}{\zeta^2}\sin\bar{\omega}_n t_1\sin\bar{\omega}_n(2t_1-t_2)\Big\}\Big\}$$

$$L_{s5}(t_1, t_2, s)|_{2t_1-t_2\geq 0}=\frac{-\zeta^2}{4\lambda(s)(\zeta^2+\lambda^2(s))}\Big\{e^{-(2st_1+h_n\omega_n(t_2-t_1))}$$
$$\cdot\Big(1+\frac{\lambda^2(s)}{\zeta^2}\Big)\sin\bar{\omega}_n(t_2-t_1)-\frac{1}{2}e^{-h_n\omega_n(t_2+t_1)}\Big\{\sin\bar{\omega}_n(t_2-t_1)$$

$$-\frac{\lambda(s)}{\zeta}\cos\bar{\omega}_n(t_2+t_1)-2\frac{\lambda^2(s)}{\zeta^2}\cos\bar{\omega}_n t_2\sin\bar{\omega}_n t_1\Big\}$$
$$-\frac{1}{2}e^{-(h_n\omega_n(t_2+t_1)-2\lambda(s)\omega_n(t_2-t_1))}\Big\{\sin\bar{\omega}_n(t_2-t_1)$$
$$+\frac{\lambda(s)}{\zeta}\cos\bar{\omega}_n(3t_1-t_2)+2\frac{\lambda^2(s)}{\zeta^2}\sin\bar{\omega}_n t_1\cos\bar{\omega}_n(2t_1-t_2)\Big\}\Big]$$

$$L_{c1}(t_1,t_2,s)|_{2t_1-t_2\leqq 0}=\frac{\zeta^2}{8\lambda(s)(\zeta^2+\lambda^2(s))}\Big[e^{-(2st_1+h_n\omega_n(t_2-t_1))}$$
$$\cdot\Big\{\cos\bar{\omega}_n(t_2-t_1)+\frac{\lambda(s)}{\zeta}\sin\bar{\omega}_n(t_2-t_1)\Big\}-e^{-h_n\omega_n(t_2+t_1)}$$
$$\cdot\Big\{\cos\bar{\omega}_n(t_2-t_1)+\frac{\lambda(s)}{\zeta}\sin\bar{\omega}_n(t_2+t_1)+2\frac{\lambda^2(s)}{\zeta^2}\sin\bar{\omega}_n t_2\sin\bar{\omega}_n t_1\Big\}\Big]$$

$$L_{c3}(t_1,t_2,s)|_{2t_1-t_2\leqq 0}=\frac{\zeta^2}{8\lambda(s)(\zeta^2+\lambda^2(s))}\Big[e^{-(2st_1+h_n\omega_n(t_2-t_1))}$$
$$\cdot\Big\{\frac{\lambda(s)}{\zeta}\cos\bar{\omega}_n(t_2-t_1)-\sin\bar{\omega}_n(t_2-t_1)\Big\}+e^{-h_n\omega_n(t_2+t_1)}$$
$$\cdot\Big\{\sin\bar{\omega}_n(t_2-t_1)-\frac{\lambda(s)}{\zeta}\cos\bar{\omega}_n(t_2+t_1)-2\frac{\lambda^2(s)}{\zeta^2}\cos\bar{\omega}_n t_2\sin\bar{\omega}_n t_1\Big\}\Big]$$

$$L_{s4}(t_1,t_2,s)|_{2t_1-t_2\leqq 0}=\frac{\zeta^2}{8\lambda(s)(\zeta^2+\lambda^2(s))}\Big[e^{-(2st_1+h_n\omega_n(t_2-t_1))}$$
$$\cdot\Big\{\cos\bar{\omega}_n(t_2-t_1)+\frac{\lambda(s)}{\zeta}\sin\bar{\omega}_n(t_2-t_1)\Big\}-e^{-h_n\omega_n(t_2+t_1)}$$
$$\cdot\Big\{\cos\bar{\omega}_n(t_2-t_1)+\frac{\lambda(s)}{\zeta}\sin\bar{\omega}_n(t_2+t_1)+2\frac{\lambda^2(s)}{\zeta^2}\sin\bar{\omega}_n t_2\sin\bar{\omega}_n t_1\Big\}\Big]$$

$$L_{s5}(t_1,t_2,s)|_{2t_1-t_2\leqq 0}=\frac{-\zeta^2}{8\lambda(s)(\zeta^2+\lambda^2(s))}\Big[e^{-(2st_1+h_n\omega_n(t_2-t_1))}$$
$$\cdot\Big\{\sin\bar{\omega}_n(t_2-t_1)-\frac{\lambda(s)}{\zeta}\cos\bar{\omega}_n(t_2-t_1)\Big\}-e^{h_n\omega_n(t_2+t_1)}$$
$$\cdot\Big\{\sin\bar{\omega}_n(t_2-t_1)-\frac{\lambda(s)}{\zeta}\cos\bar{\omega}_n(t_2+t_1)-2\frac{\lambda^2(s)}{\zeta^2}\cos\bar{\omega}_n t_2\sin\bar{\omega}_n t_1\Big\}\Big]$$

$$U_{c1}(t_1,t_2,s,s')=\frac{\zeta^2}{2(\lambda(s)+\lambda(s'))(\zeta^2+\lambda^2(s))}\Big[\{e^{-((s+s')t_1+h_n\omega_n(t_2-t_1))}$$
$$+\varkappa(2t_1-t_2)e^{-(s't_2+st_1+\lambda(s)\omega_n(t_2-t_1))}\}\{\mu_1(s,s')\cos\bar{\omega}_n(t_2-t_1)$$
$$-\mu_3(s,s')\sin\bar{\omega}_n(t_2-t_1)\}-\frac{1}{2}e^{-h_n\omega_n(t_2+t_1)}$$
$$\cdot\{2\mu_1(s,s')\cos\bar{\omega}_n t_2\cos\bar{\omega}_n t_1+2\mu_2(s,s')\sin\bar{\omega}_n t_2\sin\bar{\omega}_n t_1$$
$$-(\mu_3(s,s')-\mu_4(s,s'))\sin\bar{\omega}_n(t_2+t_1)\}$$
$$-\varkappa(2t_1-t_2)e^{-(h_n\omega_n(t_2+t_1)-2\lambda(s)\omega_n(t_2-t_1))}\{\mu_1(s,s')\cos\bar{\omega}_n t_1\cos\bar{\omega}_n(2t_1-t_2)$$
$$+\mu_2(s,s')\sin\bar{\omega}_n t_1\sin\bar{\omega}_n(2t_1-t_2)-\mu_3(s,s')\cos\bar{\omega}_n t_1\sin\bar{\omega}_n(2t_1-t_2)$$
$$+\mu_4(s,s')\sin\bar{\omega}_n t_1\cos\bar{\omega}_n(2t_1-t_2)\}\Big]$$

$$U_{c3}(t_1, t_2, s, s') = \frac{-\zeta^2}{2(\lambda(s)+\lambda(s'))(\zeta^2+\lambda^2(s))}\Big\{e^{-((s+s')t_1+h_n\omega_n(t_2-t_1))}$$
$$\cdot\{\mu_3(s, s')\cos\bar{\omega}_n(t_2-t_1)+\mu_1(s, s')\sin\bar{\omega}_n(t_2-t_1)\}$$
$$-\varkappa(2t_1-t_2)e^{-(s't_2+st_1+\lambda(s)\omega_n(t_2-t_1))}\{\mu_4(s, s')\cos\bar{\omega}_n(t_2-t_1)$$
$$+\mu_2(s, s')\sin\bar{\omega}_n(t_2-t_1)\}+\frac{1}{2}e^{-h_n\omega_n(t_2+t_1)}$$
$$\cdot\{2\mu_2(s, s')\cos\bar{\omega}_nt_2\sin\bar{\omega}_nt_1-2\mu_1(s, s')\sin\bar{\omega}_nt_2\cos\bar{\omega}_nt_1$$
$$-(\mu_3(s, s')-\mu_4(s, s'))\cos\bar{\omega}_n(t_2+t_1)\}$$
$$+\varkappa(2t_1-t_2)e^{-(h_n\omega_n(t_2+t_1)-2\lambda(s)\omega_n(t_2-t_1))}\{\mu_2(s, s')\sin\bar{\omega}_nt_1\cos\bar{\omega}_n(2t_1-t_2)$$
$$-\mu_1(s, s')\cos\bar{\omega}_nt_1\sin\bar{\omega}_n(2t_1-t_2)+\mu_3(s, s')\cos\bar{\omega}_nt_1\cos\bar{\omega}_n(2t_1-t_2)$$
$$+\mu_4(s, s')\sin\bar{\omega}_nt_1\sin\bar{\omega}_n(2t_1-t_2)\}\Big]$$

$$U_{s4}(t_1, t_2, s, s') = \frac{\zeta^2}{2(\lambda(s)+\lambda(s'))(\zeta^2+\lambda^2(s))}\Big[\{e^{-((s+s')t_1+h_n\omega_n(t_2-t_1))}$$
$$-\varkappa(2t_1-t_2)e^{-(s't_2+st_1+\lambda(s)\omega_n(t_2-t_1))}\}\{\mu_1(s, s')\cos\bar{\omega}_n(t_2-t_1)$$
$$-\mu_3(s, s')\sin\bar{\omega}_n(t_2-t_1)\}-\frac{1}{2}e^{-h_n\omega_n(t_2+t_1)}$$
$$\cdot\{2\mu_1(s, s')\cos\bar{\omega}_nt_2\cos\bar{\omega}_nt_1+2\mu_1(s, s')\sin\bar{\omega}_nt_2\sin\bar{\omega}_nt_1$$
$$-(\mu_3(s, s')-\mu_4(s, s'))\sin\bar{\omega}_n(t_2+t_1)\}$$
$$+\varkappa(2t_1-t_2)e^{-(h_n\omega_n(t_2+t_1)-2\lambda(s)\omega_n(t_2-t_1))}\{\mu_1(s, s')\cos\bar{\omega}_nt_1\cos\bar{\omega}_n(2t_1-t_2)$$
$$+\mu_2(s, s')\sin\bar{\omega}_nt_1\sin\bar{\omega}_n(2t_1-t_2)-\mu_3(s, s')\cos\bar{\omega}_nt_1\sin\bar{\omega}_n(2t_1-t_2)$$
$$+\mu_4(s, s')\sin\bar{\omega}_nt_1\cos\bar{\omega}_n(2t_1-t_2)\}\Big]$$

$$U_{s5}(t_1, t_2, s, s') = \frac{-\zeta^2}{2(\lambda(s)+\lambda(s'))(\zeta^2+\lambda^2(s))}\Big\{e^{-((s+s')t_1+h_n\omega_n(t_2-t_1))}$$
$$\cdot\{\mu_3(s, s')\cos\bar{\omega}_n(t_2-t_1)+\mu_1(s, s')\sin\bar{\omega}_n(t_2-t_1)\}$$
$$+\varkappa(2t_1-t_2)e^{-(s't_2+st_1+\lambda(s)\omega_n(t_2-t_1))}\{\mu_4(s, s')\cos\bar{\omega}_n(t_2-t_1)$$
$$+\mu_2(s, s')\sin\bar{\omega}_n(t_2-t_1)\}-\frac{1}{2}e^{-h_n\omega_n(t_2+t_1)}$$
$$\cdot\{2\mu_1(s, s')\sin\bar{\omega}_nt_2\cos\bar{\omega}_nt_1-2\mu_2(s, s')\cos\bar{\omega}_nt_2\sin\bar{\omega}_nt_1$$
$$+(\mu_3(s, s')-\mu_4(s, s'))\cos\bar{\omega}_n(t_2+t_1)\}$$
$$+\varkappa(2t_1-t_2)e^{-(h_n\omega_n(t_2+t_1)-2\lambda(s)\omega_n(t_2-t_1))}\{\mu_1(s, s')\cos\bar{\omega}_nt_1\sin\bar{\omega}_n(2t_1-t_2)$$
$$-\mu_2(s, s')\sin\bar{\omega}_nt_1\cos\bar{\omega}_n(2t_1-t_2)+\mu_3(s, s')\sin\bar{\omega}_nt_1\sin\bar{\omega}_n(2t_1-t_2)$$
$$+\mu_4(s, s')\cos\bar{\omega}_nt_1\cos\bar{\omega}_n(2t_1-t_2)\}\Big]$$

$$\mu_1(s, s') = \{\alpha_1(s, s')\alpha_5(s, s')+\alpha_2(s, s')\alpha_6(s, s')\}/\mu_0(s, s')$$
$$\mu_2(s, s') = \{\alpha_3(s, s')\alpha_5(s, s')+\alpha_4(s, s')\alpha_6(s, s')\}/\mu_0(s, s')$$
$$\mu_3(s, s') = \{\alpha_2(s, s')\alpha_5(s, s')-\alpha_1(s, s')\alpha_6(s, s')\}/\mu_0(s, s')$$
$$\mu_4(s, s') = \{\alpha_4(s, s')\alpha_5(s, s')-\alpha_3(s, s')\alpha_6(s, s')\}/\mu_0(s, s')$$
$$\mu_0(s, s') = (4\zeta^2-\lambda^2(s)+\lambda^2(s'))^2+16\zeta^2\lambda^2(s)$$

$$\alpha_1(s,s')=2\zeta^2-\lambda^2(s)+\lambda(s)\lambda(s'),\quad \alpha_2(s,s')=\zeta(3\lambda(s)-\lambda(s'))$$
$$\alpha_3(s,s')=2\zeta^2-4\lambda^2(s)-\lambda(s)\lambda(s')+\lambda^2(s')$$
$$\alpha_4(s,s')=\zeta(5\lambda(s)+\lambda(s'))-\frac{\lambda(s)}{\zeta}(\lambda^2(s)-\lambda^2(s'))$$
$$\alpha_5(s,s')=4\zeta^2-5\lambda^2(s)+\lambda^2(s'),\quad \alpha_6(s,s')=\frac{\lambda(s)}{\zeta}(8\zeta^2-\lambda^2(s)+\lambda^2(s'))$$
$$\varkappa(t)=\begin{cases}1, & t>0\\ 0, & t\leqq 0\end{cases}$$

Numerical computation for Eqs. (13) and (14) have been carried out for the set of parameters $st_m=0.4$, $\tau/T_0=3$, 10, 20, $h_n=0.02$, 0.05, 0.1, 0.2 and $h_0=0.9$. The value of h_0 determines the peak sharpness of $S_y(\omega)$. As could be expected, h_0 would vary with the site conditions, and, in many cases, from earthquake to earthquake. Throughout this study, however, we shall keep h_0 fixed at 0.9, which was determined in connection with the values of the mean response spectra as will be explained and discussed later, in chapter 6.

The results of computation are plotted in Figs. 3 and 4. Fig. 3 shows the time variation of the r.m.s. response, in which $\sigma_y(t)\omega_n^2/\beta$ and $\sigma_{\dot{y}}(t)\omega_n/\beta$ are so close that they are inseparable. It may be observed that the maximum value of the r.m.s. response takes place later than the time t_m of the maximum intensity of excitation. It is obvious that this result is partly attributable to the vibrational characteristics of the structure which are manifest in the unit impulse response $h(t)$ in Eq. (8); i.e., the response assumes its maximum value necessarily later than the excitation. It is obvious that this effect is remarkable in structures with longer natural periods; this is also true for a shorter duration of the excitation. Indeed, the former statement is justified by Fig. 3(b) and the latter by Fig. 3(a). In addition, this time lag is greatly affected by the damping factor h_n. When a structure initially at reat is subjected to random excitation, its r.m.s. response increases until the rate of energy dissipation due to the structural damping copes with the mean energy delivered by the cxcitation per unit time. Thus, it follows that if h_n is small, $\sigma_y(t)$ continues to increase for the time being even after the excitation level $f(t;\tau)$ has begun to decrease as shown in Fig. 3(a). These results demonstrate that a transient effect is present to a considerable extent in the case of non-stationary earthquake excition, but with the intensity of response varying slowly compared with the case of sudden action of a stationary excitation.[10]

Smooth curves in Fig. 3 imply that Eqs. (13) may further be closely approximated by neglecting the sinusoidal members and the higher order terms in h_n in the formulae, which reduces Eq. (13) to the following simple form:

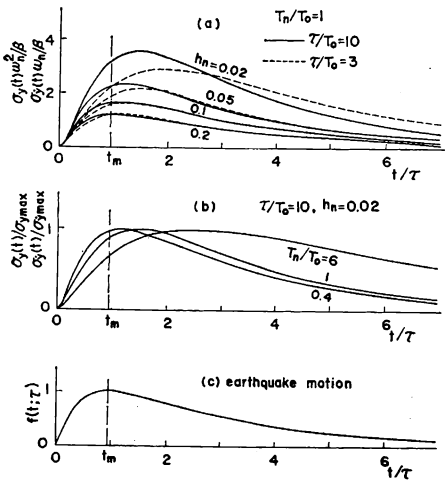

Fig. 3. r.m.s. Responses (Standard Deviation) to Earthquake.

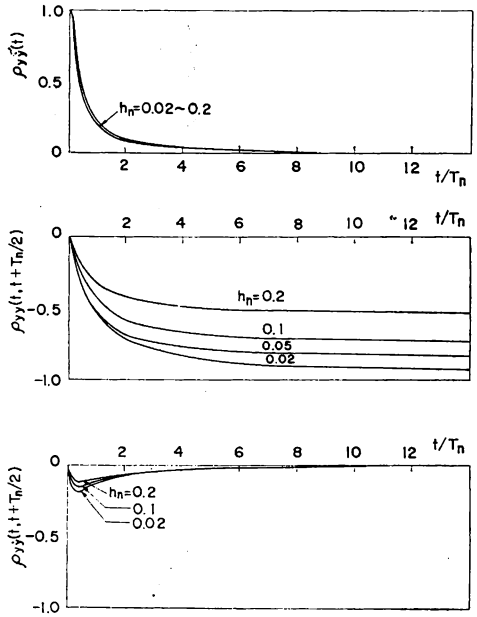

Fig. 4. Correlation Coefficients of Earthquake Response ($\tau/T_0=10$).

$$\left.\begin{aligned}\sigma_y^2(t)&\cong\frac{\pi\beta^2A^2}{4\omega_n{}^3}S_g(\omega_n)e_1(t)\\ \sigma_{\dot y}^2(t)&\cong\frac{\pi\beta^2A^2}{4\omega_n}S_g(\omega_n)e_1(t)=\omega_n{}^2\sigma_y^2(t)\end{aligned}\right\}\qquad\cdots\cdots\cdots\cdots(15)$$

where

$$e_1(t)=\frac{e_0(s,s,t)}{\lambda(s)}+\frac{e_0((1+\xi)s,(1+\xi)s,t)}{\lambda((1+\xi)s)}-\frac{2}{\lambda(s)+\lambda((1+\xi)s)}\cdot\{e_0(s,(1+\xi)s,t)+e_0((1+\xi)s,s,t)\}$$

$$e_0(s,s',t)=e^{-(s+s')t}-e^{-2h_n\omega_nt}$$

Indeed, the numerical values of $\sigma_y(t)$ and $\sigma_{\dot y}(t)$ from Eq. (15) are sufficiently close to those in Fig. 3. The same simplification is also possible for the correlation coefficients in Eq. (14). However, the resulting formulae proved not necessarily to give sufficiently accurate numerical values.

As a measure of the intensity of the nonstationary response, the maximum value $\sigma_{y\max}$ of $\sigma_y(t)$ is shown in Fig. 5 in a form similar to that of the response spectra.

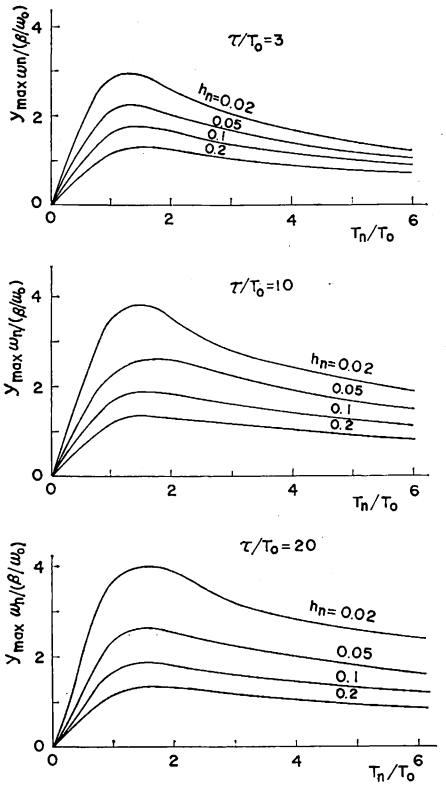

Fig. 5. Maximum r.m.s. Response.

4. Probability Distribution of the Maximum Response from the Pure-Birth-Process Equation

(1) Basic Solution

Let Y denote the maximum absolute value of the response $y(t)$ in the duration considered. Then the probability distribution $\Phi(Y)$ of Y is represented by

$$\Phi(Y)=\mathrm{P}[\max|y(t)|\leqq Y;\ 0\leqq t\leqq\infty] \qquad \cdots\cdots(16)$$

Eq. (16) can be formulated in terms of the fundamental differential equation of the pure-birth-process[7~9], from which we obtain

$$\Phi(Y)=a_0(Y)\exp\left\{-\int_0^\infty c_0(Y,t)dt\right\} \qquad \cdots\cdots(17)$$

where

$$a_0(Y)=\mathrm{P}[|y(0)|\leqq Y]$$

$$c_0(Y,t)dt=\frac{\mathrm{P}[|y(t+dt)|>Y\cap\max|y(t')|\leqq Y;\ 0\leqq t'\leqq t]}{\mathrm{P}[\max|y(t')|\leqq Y;\ 0\leqq t'\leqq t]} \qquad \cdots\cdots(18)$$

(2) **Approximate Solution**

The solution for the probability distribution $\Phi(Y)$ of the maximum response given in Eq. (17) cannot be represented in an explicit form since it is extremely difficult to obtain an explicit expression for $c_0(Y,t)$ in Eq. (18) due to the correlation between responses at different times on the continuous time axis. Therefore, we shall make an approximation to Eq. (18) in a manner more general than those in the former studies cited in Chapter 1.

In the exact solution, Eq. (18), is required to hold throughout the continuous time axis. Here, let $\bar{c}_0(Y,t)$ satisfy Eq. (18) only at discrete instants $t_1, t_2\cdots\cdots, t_r\, t$ such that

$$0\leqq t_1<t_2\cdots\cdots<t_r<t$$

Namely, we set

$$\bar{c}_0(Y,t)dt=\frac{\mathrm{P}[\{|y(t+dt)|>Y\cap|y(t)|\leqq Y\}\cap\{\bigcap_{k=1}^{r}|y(t_k)|\leqq Y\}]}{\mathrm{P}[|y(t)|\leqq Y\cap\{\bigcap_{k=1}^{r}|y(t_k)|\leqq Y\}]}=\frac{Q_1(Y,t)}{Q_2(Y,t)}dt \qquad \cdots\cdots(19)$$

where

$$Q_1(Y,t)dt=\mathrm{P}[\{|y(t+dt)|>Y\cap|y(t)|\leqq Y\}\cap\{\bigcap_{k=1}^{r}|y(t_k)|\leqq Y\}]$$

$$Q_2(Y,t)dt=\mathrm{P}[|y(t)|\leqq Y\cap\{\bigcap_{k=1}^{r}|y(t_k)|\leqq Y\}]$$

If we let $\bar{c}_0(Y,t)$ in Eq. (19) approximate $c_0(Y,t)$, then an approximate formula for Eq. (17) is obtained as

$$\Phi(Y)\cong a_0(Y)\exp\left\{-\int_0^{\infty}\bar{c}_0(Y,t)dt\right\} \qquad \cdots\cdots(20)$$

In Eqs. (19) and (20), the effect of correlation between the response at different times is taken into account, though in an approximate manner, which describes the phenomenon more precisely than the simple approximation of of the independence of the response from its past history adopted in earlier papers on the maximum response. The approximation of history-independence of response is contained in Eqs. (19) and (20) as a specific case of $r=0$. In the subsequent discussions, this case shall be referred to as the first approximation, the case of $r=1$, as the second approximation, and so on. The approximation error is expected to reduce with increasing values of r.

Next, $Q_1(Y,t)$ and $Q_2(Y,t)$ in Eq. (19) shall be represented in a more

explicit form. Set, for simplicity, $y(t_1)=y_1$, $y(t_2)=y_2$, ……, $y(t_r)=y_r$, $y(t)=y_t$, $\dot{y}(t)=\dot{y}_t$. On applying the method of analysis of the threshold-value crossing problem developed by S. O. Rice[16] to the present multi-dimensional random variables, $Q_1(Y,t)$ and $Q_2(Y,t)$ are reduced to

$$Q_1(Y,t)=\frac{\sigma_v}{\sigma_t}\int_{-Y/\sigma_1}^{Y/\sigma_1}d\xi_1\int_{-Y/\sigma_2}^{Y/\sigma_2}d\xi_2\cdots\cdots\int_{-Y/\sigma_r}^{Y/\sigma_r}\left\{\int_{-\infty}^{0}|\dot{\xi}_t|\phi_{1n}\left(\xi_1,\xi_2,\cdots\right.\right.$$
$$\left.\cdots\cdots,\xi_r,-\frac{Y}{\sigma_t},\dot{\xi}_t\right)d\dot{\xi}_t$$
$$\left.+\int_0^{\infty}\dot{\xi}_t\phi_{1n}\left(\xi_1,\xi_2\cdots\cdots,\xi_r,\frac{Y}{\sigma_t},\dot{\xi}_t\right)d\dot{\xi}_t\right\}d\xi_r \qquad \cdots\cdots(21)$$

$$Q_2(Y,t)=\int_{-Y/\sigma_1}^{Y/\sigma_1}d\xi_1\int_{-Y/\sigma_2}^{Y/\sigma_2}d\xi_2\cdots\cdots\int_{-Y/\sigma_r}^{Y/\sigma_r}d\xi_r\int_{-Y/\sigma_t}^{Y/\sigma_t}\phi_{2n}(\xi_1,\xi_2,\cdots\cdots,\xi_r,\xi_t)d\xi_t \qquad \cdots\cdots(22)$$

In which $\phi_{1n}(\xi_1,\xi_2,\cdots\cdots,\xi_r,\xi_t,\dot{\xi}_t)$ and $\phi_{2n}(\xi_1,\xi_2,\cdots\cdots,\xi_r,\xi_t)$ are the joint probability density functions of the nondimensional variables $\xi_1,\xi_2,\cdots\cdots,\xi_r,\xi_t,\dot{\xi}_t$ and $\xi_1,\xi_2,\cdots\cdots,\xi_r,\xi_t$ defined by

$$\xi_i=y_i/\sigma_i\,;\ (i=1,2,\cdots\cdots,r),\quad \xi_t=y_t/\sigma_t,\quad \dot{\xi}_t=\dot{y}_t/\sigma_v$$
$$\sigma_i=\{\mathrm{E}[y_i^2]\}^{1/2}\,;\ (i=1,2,\cdots\cdots,r),\quad \sigma_t=\{\mathrm{E}[y_t^2]\}^{1/2},\quad \sigma_v=\{\mathrm{E}[\dot{y}_t^2]\}^{1/2}$$

The joint probability density functions in Eqs. (21) and (22) may take arbitrary forms, out of which the typical case of the normal distribution which is of primary importance in application shall be described below.

When a linear structure is subjected to an excitation represented by a random process with a normal distribution, white or non-white, its response also has a normal distribution since an arbitrary linear combination of normal random variables is normal as well. Hence, in such a case the joint probability density functions in Eqs. (21) and (22) become multi-dimensional normal distributions with respect to each of their independent variables. Furthermore, for the normal distribution, the number of multiple integrations representing $Q_1(Y,t)$ and $Q_2(Y,t)$ can be reduced analytically by one, in which case Eq. (20) is rewritten as

$$\Phi(Y,t)\cong\mathrm{erf}\left(\frac{Y}{\sqrt{2}\,\sigma_0}\right)\exp\left\{-\int_0^{\infty}\bar{c}_0(Y,t)dt\right\} \qquad \cdots\cdots(23)$$

where

$$\bar{c}_0(Y,t)=Q_1(Y,t)/Q_2(Y,t),\quad \sigma_0=\{\mathrm{E}[y^2(0)]\}^{1/2}$$

$Q_1(Y,t)$ and $Q_2(Y,t)$ in Eqs. (21) and (22) for the normal distribution yield

$$Q_1(Y,t)=\frac{1}{\mu_{vv}\sqrt{(2\pi)^{r+2}C_1}}\frac{\sigma_v}{\sigma_t}\exp\left\{-\frac{1}{2}\left(\mu_{tt}-\frac{\mu^2_{tv}}{\mu_{vv}}\right)\left(\frac{Y}{\sigma_t}\right)^2\right\}$$

$$\times\int_{-Y/\sigma_1}^{Y/\sigma_1}d\xi_1\int_{-Y/\sigma_2}^{Y/\sigma_2}d\xi_2\cdots\cdots\int_{-Y/\sigma_r}^{Y/\sigma_r}\left[\exp\left(-\frac{u_1}{2}\right)\left\{\exp\left(-\frac{{v_1}^2}{2}\right)+\sqrt{\frac{\pi}{2}}v_1\left(1+\mathrm{erf}\left(\frac{v_1}{\sqrt{2}}\right)\right)\right\}+\exp\left(-\frac{u_2}{2}\right)\left\{\exp\left(-\frac{{v_2}^2}{2}\right)+\sqrt{\frac{\pi}{2}}v_2\left(1+\mathrm{erf}\left(\frac{v_2}{\sqrt{2}}\right)\right)\right\}\right]d\xi_r$$

in which

$$u_1=u_1(\xi_1,\xi_2,\cdots\cdots,\xi_r)=\sum_{i=1}^{r}\sum_{j=1}^{r}\mu_{ij}\xi_i\xi_j-\frac{1}{\mu_{vv}}\left(\sum_{i=1}^{r}\mu_{iv}\xi_i\right)^2+2\left\{\sum_{i=1}^{r}\left(\mu_{it}-\frac{\mu_{tv}\mu_{iv}}{\mu_{vv}}\right)\xi_i\right\}\left(\frac{Y}{\sigma_t}\right)$$

$$u_2=u_2(\xi_1,\xi_2,\cdots\cdots,\xi_r)=\sum_{i=1}^{r}\sum_{j=1}^{r}\mu_{ij}\xi_i\xi_j-\frac{1}{\mu_{vv}}\left(\sum_{i=1}^{r}\mu_{iv}\xi_i\right)^2-2\left\{\sum_{i=1}^{r}\left(\mu_{it}-\frac{\mu_{tv}\mu_{iv}}{\mu_{vv}}\right)\xi_i\right\}\left(\frac{Y}{\sigma_t}\right)$$

$$v_1=v_1(\xi_1,\xi_2,\cdots\cdots,\xi_r)=-\frac{1}{\sqrt{\mu_{vv}}}\left(\mu_{tv}\frac{Y}{\sigma_t}+\sum_{i=1}^{r}\mu_{iv}\xi_i\right)$$

$$v_2=v_2(\xi_1,\xi_2,\cdots\cdots,\xi_r)=-\frac{1}{\sqrt{\mu_{vv}}}\left(\mu_{tv}\frac{Y}{\sigma_t}-\sum_{i=1}^{r}\mu_{iv}\xi_i\right)$$

$C_1=\det \boldsymbol{C}_1$, $[\mu_{ij}]=\boldsymbol{C}_1^{-1}$

$\mu_{it}=\mu_{ti}=\mu_i$, $_{r+1}=\mu_{r+1}$, $_i$, $\mu_{iv}=\mu_{vi}=\mu_i$, $_{r+2}=\mu_{r+2}$, $_i$

$\mu_{tv}=\mu_{vt}=\mu_{r+1}$, $_{r+2}=\mu_{r+2}$, $_{r+1}$, $\mu_{tt}=\mu_{r+1}$, $_{r+1}$, $\mu_{vv}=\mu_{r+2}$, $_{r+2}$

$$\boldsymbol{C}_1=\begin{pmatrix}1&\rho_{12}&\cdots\cdots&\rho_{1r}&\rho_{1t}&\rho_{1v}\\ \rho_{21}&1&\cdots\cdots&\rho_{2r}&\rho_{2t}&\rho_{2v}\\ \vdots&&&\vdots&\vdots&\\ \rho_{r1}&\rho_{r2}&\cdots\cdots&1&\rho_{rt}&\rho_{rv}\\ \rho_{t1}&\rho_{t2}&\cdots\cdots&\rho_{tr}&1&\rho_{tv}\\ \rho_{v1}&\rho_{v2}&\cdots\cdots&\rho_{vr}&\rho_{vt}&1\end{pmatrix}$$

$\rho_{ij}=\rho_{ji}=\mathrm{E}[\xi_i\xi_j]$, $\rho_{it}=\rho_{ti}=\mathrm{E}[\xi_i\xi_t]$

$\rho_{iv}=\rho_{vi}=\mathrm{E}[\xi_i\dot{\xi}_t]$, $\rho_{tv}=\rho_{vt}=\mathrm{E}[\xi_t\dot{\xi}_t]$

and

$$Q_2(Y,t)=\frac{1}{2\sqrt{(2\pi)^r\kappa_{tt}C_0}}\int_{-Y/\sigma_1}^{Y/\sigma_1}d\xi_1\int_{-Y/\sigma_2}^{Y/\sigma_2}d\xi_2\cdots\cdots\int_{-Y/\sigma_r}^{Y/\sigma_r}\exp\left(-\frac{u_0}{2}\right)\cdot\left\{\mathrm{erf}\left(\frac{\sqrt{\kappa_{tt}}\frac{Y}{\sigma_t}+v_0}{\sqrt{2}}\right)+\mathrm{erf}\left(\frac{\sqrt{\kappa_{tt}}\frac{Y}{\sigma_t}-v_0}{\sqrt{2}}\right)\right\}d\xi_r$$

in which

$$u_0=u_0(\xi_1,\xi_2,\cdots\cdots,\xi_r)=\sum_{i=1}^{r}\sum_{j=1}^{r}\kappa_{ij}\xi_i\xi_j-{v_0}^2$$

$$v_0=v_0(\xi_1, \xi_2, \cdots\cdots, \xi_r)=-\frac{1}{\sqrt{\kappa_{tt}}}\sum_{i=1}^{r}\kappa_{it}\xi_i$$

$$C_0=\det \boldsymbol{C}_0, \quad [\kappa_{ij}]=\boldsymbol{C}_0^{-1}, \quad \kappa_{it}=\kappa_{ti}=\kappa_{i,\,r+1}=\kappa_{r+1,\,i}, \quad \kappa_{tt}=\kappa_{r+1,\,r+1}$$

$$\boldsymbol{C}_0=\begin{pmatrix} 1 & \rho_{12} & \cdots\cdots & \rho_{1r} & \rho_{1t} \\ \rho_{21} & 1 & \cdots\cdots & \rho_{2r} & \rho_{2t} \\ \vdots & & & \vdots & \\ \rho_{r1} & \rho_{r2} & \cdots\cdots & 1 & \rho_{rt} \\ \rho_{t1} & \rho_{t2} & \cdots\cdots & \rho_{tr} & 1 \end{pmatrix}$$

For specific cases of $r=0, 1$, the expressions for $Q_1(Y, t)$ and $Q_2(Y, t)$ are somewhat simplified[9,14].

The expected value $\mathrm{E}[Y]$ of the maximum response can be represented in the following form analogous to Eq. (3):

$$\mathrm{E}[Y]=\int_0^\infty\{1-\Phi(Y)\}dY \qquad \cdots\cdots\cdots\cdots(24)$$

(3) Numerical Results and Discussion

By use of the variances and the correlation coefficients of the response obtained in 3, numerical values have been computed for the probability distribution $\Phi(Y)$ of the maximum deformation Y in response to a nonstationary Gaussian random excitation of the earthquake type, with the aid of the approximate formula (23) derived from the pure-birth-process method for the various values of the parameters h_n, T_n/T_0, and τ/T_0. The second approximation, $r=1$, has been adopted and the time t_1 to introduce the correlation effects of the response was taken as

$$t_1=t-\frac{T_n}{2}$$

from the results of the approximation error survey.[9]

Along with the analytical procedure, numerical simulation of the maximum response Y has been carried out. For each set of parameters, 40~50 sample accelerograms have been generated, from which the experimental probability distribution has been obtained as the cumulative probability of the maximum structural response to them.

Some numerical examples of the analytical and the simulated results are shown in Figs. 6~8. From these figures, it is obvious that the discrepancy between the analytical and simulated results grows greater with increasing T_n/T_0 and with decreasing τ/T_0 and h_n. For $\tau/T_0=3$ and $T_n/T_0=1, 4$, Fig. 6, fairly good agreement between the analytical and simulated results seems to attained only for $h_n=0.2$ and an extremely high level of Y for lower damping

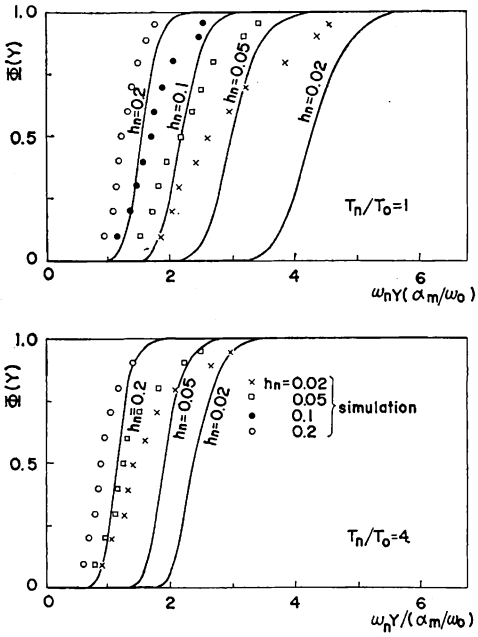

Fig. 6. Probability Distribution of the Maximum Earthquake Response Based on the Pure-Birth-Process Method (τ/T_0 =3).

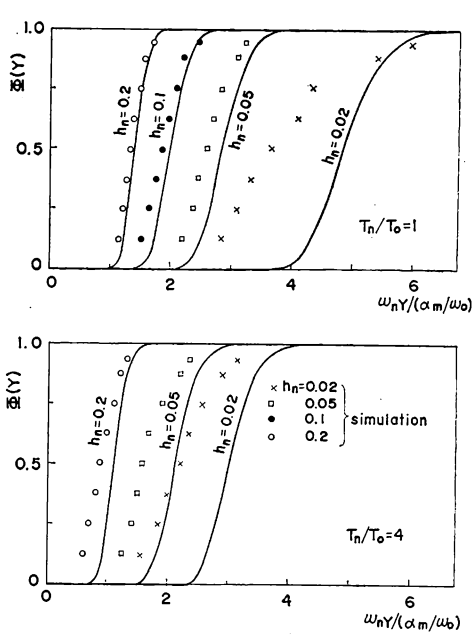

Fig. 7. Probability Distribution of the Maximum Earthquake Response Based on the Pure-Birth-Process Method (τ/T_0 =10).

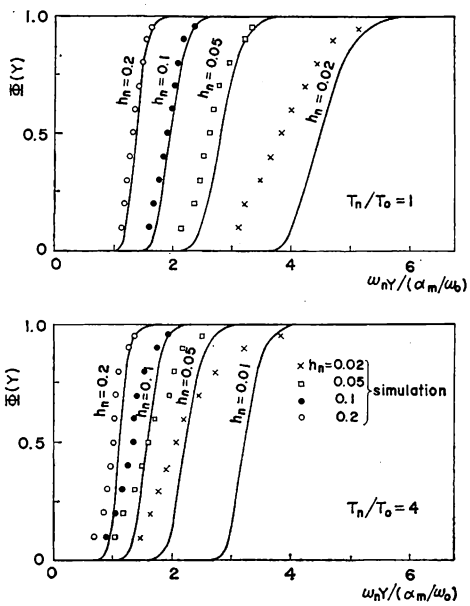

Fig. 8 Probability Distribution of the Maximum Earthquake Response Based on the Pure-Birth-Process Method (τ/T_0=20).

factors. This result is considered to be a consequence of the approximation procedure which was adopted in the pure-birth-process method, and it would demonstrate that a careful choice of parameters must be made in applying this method to the problem of the statistics of the maximum earthquake response. These error characteristics could be explained in the following manner.

i) The pure-birth-process method so far discussed takes account of the correlation effects between the responses only at a limited number of discrete times, though it has been improved if compared with the former studies with the history-independence assumption. As a matter of fact, however, it is excessively time consuming to carry out numerical computations with a high order of approximation, say $r=3, 4$ or more. Hence, if the damping factor h_n is very small and there occurs as a consequence a high correlation between the responses at times separated by several times the natural period, then pure-birth-process method fails practically to be applicable with a sufficient accuracy.

ii) A great part of the error due to a small h_n is considered to be caused by the subsiding tail of the r.m.s. response σ_y for a large t. It was pointed out in 3. (2) that when σ_y attains its maximum value and begins clearly to decrease, the excitation level $f(t;\tau)$ has already decreased to a considerable extent if h_n is small. Hence in such a case, the subsiding tail of $\sigma_y(t)$ is considered to represent primarily the effect of damped free vibration, and the maximum response is expected to occur exclusively in a relatively short time interval containing the maximum of $\sigma_y(t)$. However, due to the procedure which, starting from the exact solution Eq. (17), led to the approximate formula (20), this subsiding tail has in effect been treated as though it possessed a more random nature which might affect the maximum response. In this sense, if h_n is so small that this kind of error grows large, the pure-birth-process method will overestimate the maximum response, and Eq. (14) will give a lower bound of the probability distribution $\Phi(Y)$. Indeed the results for $h_n=0.02$ in Figs. 6~8, for example, seem to support these arguments.

iii) If T_n/T_0 is very large or τ/T_0 is very small, which implies that the input is impulsive rather than a continuous excitation of slowly varying intensity, then the maximum value of $\sigma_y(t)$ appears much later than that of the excitation, as we observed in Fig. 3, the case of $T_n/T_0=6$, for example. Then, analogous to the discussion in ii), the r.m.s. response following this maximum value is also considered to represent the subsiding tail due to free vibration, not the effect of forced vibration. Thus, large T_n/T_0 and small τ/T_0 also have the same effects as small h_n and tend to increase the approximation error in

$\Phi(Y)$.

From the foregoing discussions on the accuracy of the approximate procedure, it would be obvious that the pure-birth-process method so far developed furnishes a good approximation to the probability distribution of the maximum response for a limited range of parameters; i.e., for larger h_n and τ/T_0, and smaller T_n/T_0. If we admit the judgment that the analytical and simulated values for $h_n=0.05$ and $T_n/T_0=1$ in Fig. 7 are in appreciable agreement and let them give a limiting degree of tolerable error for practical use, we can separate the successful portion of the whole analytical results.[14] The range of parameters in which the pure-birth-process method is applicable in the sense of the above statement is shown in Fig. 9. The domain on the "A" side of each curve corresponding to the probability levels $\Phi(Y)$ is the area

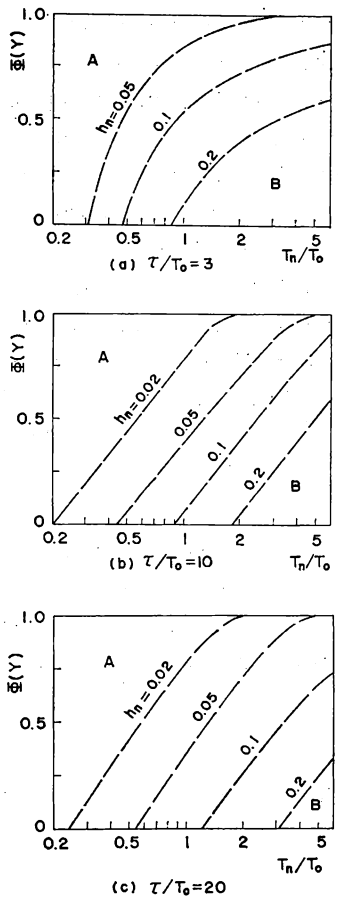

Fig. 9. Precision Zoning for the Pure-Birth-Process Method.

where the pure-birth-process method is valid and that on the "B" side is where it fails to be. In the case of Fig. 9(b), for example, the pure-birth-process method is applicable to structures with $h_n=0.1$ and $T_n/T_0=2$ in the range $\Phi(Y)>0.4$. It should be noted, however, that these curves are only representative of error criteria, and we should understand that the error caused by the approximation changes rapidly but continuously somewhere about them.

A more reasonable method of analysis for the range of parameters in the "B" domain is discussed in the next chapter in connection with the peak envelope distribution.

5. Probability Distribution of the Maximum Earthquake Response in Terms of the Peak Envelope Distribution

(1) Analytical Procedure

It has been shown in the previous chapter that when the pure-birth-process method for analyzing the maximum structural response is applied to the problem of earthquake-type excitation, its approximation error tends to be large in some ranges of ruling parameters. Hence for such ranges of parameters, there is required an alternative method of analysis.

It was pointed out in 4. (3) that the approximate formula Eq. (20) fails to be accurate when the subsiding tail of the r.m.s. response $\sigma_y(t)$ for a large t primarily represents the effect of the damped free vibration and does not contribute to the maximum response. Thus, in discussing the maximum response for such cases, it is desirable to adopt a method which evaluates exclusively a relatively short interval of time in which the maximum value $\sigma_{y\max}$ of $\sigma_y(t)$ takes place. In this chapter, we shall employ the peak envelope distribution developed by S. O. Rice[16] as such a method and apply it to our present problem.

It is obvious both from the foregoing discussion and from evidence shown by many authors that the random response $y(t)$ of a slightly damped linear structure, the object of analysis throughout this study, can be treated as a sinusoidal time function with a slowly varying random amplitude $A(t)$ and a random phase angle $\phi(t)$; i.e.,

$$y(t)=A(t)\sin(\omega_n t+\phi(t))$$

as illustrated in Fig. 10. The envelope $W(t)$ is given by

$$W(t)=\left\{y^2(t)+\frac{\dot{y}^2(t)}{\omega_n{}^2}\right\}^{1/2}\cong A(t)$$

The slowly varying envelope $W(t)$ is also a random process and takes on

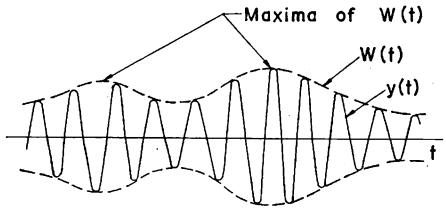

Fig. 10. Illustration of Amplitude $y(t)$, Envelope $W(t)$, and Peak Envelope (Maxima of $W(t)$).

maxima and minima from time to time. Such maxima, or peak envelopes*, are considered to be the maximum values of $|y(t)|$ in the time interval in which only a single peak envelope is contained. Since, as discussed above, the subject of this chapter is the maximum response determined exclusively in a relatively short time interval in which $\sigma_y(t)$ attains its maximum value, it would be appropriate to let a peak envelope taking place in or in the vicinity of such an interval represent the maximum response Y.

The probability distribution of the peak envelope of a narrow-band stationary Gaussian process has been discussed by S. O. Rice[16] from which the solution was derived in an explicit form for a process with a power spectrum symmetrical about its mid-band frequency. Although the structural response discussed herein is nonstationary, we shall employ Rice's result as an approximate expression for the probability distribution of the maximum response Y. For, in the time interval in which $\sigma_y(t)$ assumes its maximum value $\sigma_{y\max}$, $\sigma_y(t)$ and other statistical parameters of the response assume nearly constant values and, among them, $\rho_{y\dot{y}}(t)$ almost vanishes, thus proving that $y(t)$ is almost stationary in this interval which is of interest to us in this chapter.

Thus on applying Rice's result on the peak envelope distribution[16] to the present problem, we obtain the probability density of the maximum response in the following form:

$$\phi_E(Y)=\frac{1}{4\sigma_{ym}}\left\{\frac{32a^5z^3}{a^2-1}\left(\frac{Y}{\sigma_{ym}}\right)^3\right\}^{1/2}\exp\left\{-a^2z^2\left(\frac{Y}{\sigma_{ym}}\right)^2\right\}$$
$$\times\sum_{n=0}^{\infty}\frac{z^nA_n}{\Gamma\left(\frac{n}{2}+\frac{7}{4}\right)}\left(\frac{Y}{\sigma_{ym}}\right)^n\Big/\sum_{n=0}^{\infty}\frac{\Gamma\left(\frac{n}{2}+\frac{5}{4}\right)A_n}{\Gamma\left(\frac{n}{2}+\frac{7}{4}\right)a^n} \qquad \cdots\cdots(25)$$

where

* This terminology shall be used hereafter.

$$A_n=\begin{cases}1; & n=0\\ n+1+\sum_{m=1}^{n}\dfrac{\left(\frac{1}{2}\right)\left(\frac{3}{2}\right)\cdots\cdots\left(m-\frac{1}{2}\right)}{m!}(n-m+1)b^m; & n\geqq 1\end{cases}$$

$$b=\frac{1}{2}(3-a^2)\,;\quad a=\frac{\sqrt{b_4}}{b_2}\sigma_{ym}$$

$$z=\frac{b_2}{\sqrt{2(\sigma^2_{ym}b_4-b_2{}^2)}}$$

$$b_k=\int_0^\infty(\omega-\omega_n)^k\bar{S}_y(\omega)d\omega\,;\quad k=2,4$$

and $\Gamma(x)$ is the gamma function.

The probability distribution of the maximum response is then given by

$$\Phi(Y)\cong\Phi_E(Y)=\int_0^Y\Phi_E(Y)dY \qquad \cdots\cdots\cdots\cdots(26)$$

In Eq. (25), σ_{ym} is to assume some representative value of σ_y in the time interval of highest response level. $\bar{S}_y(\omega)$ should in principle coincide with the power spectrum $S_y(\omega)$ of the response in this time interval. However, since Eq. (25) is valid only for a power spectrum symmetrical about its mid-band frequency, we need to represent $\bar{S}_y(\omega)$ by some suitable function and let it simulate the response power spectrum. Determination of $\bar{S}_y(\omega)$ is discussed below, and σ_{ym} is determined in the next section.

The power spectrum $S_y(\omega)$ of the response $y(t)$ in the time interval in discussion is closely approximated by

$$S_y(\omega)=\frac{4h_n}{\pi\omega_n}\frac{\sigma^2_{ym}}{H(\omega)} \qquad \cdots\cdots\cdots\cdots(27)$$

where

$$H(\omega)=\left\{1-\left(\frac{\omega}{\omega_n}\right)^2\right\}^2+4h_n{}^2\left(\frac{\omega}{\omega_n}\right)^2$$

The coefficient on the right-hand side of Eq. (27) has been determined so that

$$\int_0^\infty S_y(\omega)d\omega=\sigma^2_{ym} \qquad \cdots\cdots\cdots\cdots(28)$$

$S_y(\omega)$ has its peak at $\omega=\sqrt{1-2h_n{}^2}\omega_n\cong\omega_n$ for which we have

$$S_y(\sqrt{1-2h_n{}^2}\omega_n)=\frac{\sigma^2_{ym}}{\pi h_n(1-h_n{}^2)\omega_n}\cong\frac{\sigma^2_{ym}}{\pi h_n\omega_n}=S_y(\omega_n) \qquad \cdots\cdots\cdots\cdots(29)$$

For such $S_y(\omega)$, the simulating spectral function $\bar{S}_y(\omega)$ shall be represented in the form

$$\bar{S}_y(\omega)=\frac{\nu}{\omega_n}\exp\left\{-\frac{1}{\gamma^4}\left(\frac{\omega}{\omega_n}-1\right)^4\right\} \qquad \cdots\cdots\cdots\cdots(30)$$

for which ν and γ are to be determined later. This form was chosen to make it vary in the same manner as $S_y(\omega)$ near the spectral peak; i.e., as a polynomial function of degree four in ω. $\bar{S}(\omega)$ in Eq. (30) is symmetrical about its midband frequency ω_n. The parameters ν and γ are determined by reference to Eqs. (28) and (29); i.e.,*

$$\int_{-\infty}^{\infty} \bar{S}_y(\omega)d\omega=\sigma^2{}_{ym}$$

and

$$\bar{S}_y(\omega_n)=\frac{\sigma^2{}_{ym}}{\pi h_n\omega_n}$$

From these conditions we obtain

$$\nu=\frac{\sigma^2{}_{ym}}{\pi h_n},\quad \gamma=\frac{2\pi h_n}{\Gamma\left(\frac{1}{4}\right)} \qquad \cdots\cdots\cdots\cdots(31)$$

By use of Eqs. (30) and (31), the parameters necessary for evaluation of Eqs. (25) and (26) are obtained as

$$b_2=\frac{\nu\gamma^3\omega_n{}^2}{2}\Gamma\left(\frac{3}{4}\right),\quad b_4=\frac{\nu\gamma^5\omega_n{}^4}{2}\Gamma\left(\frac{5}{4}\right)$$

$$z=1\Big/\left[\Gamma\left(\frac{3}{4}\right)\left\{2\left(\Gamma\left(\frac{1}{4}\right)\Gamma\left(\frac{5}{4}\right)-\Gamma^2\left(\frac{3}{4}\right)\right)\right\}^{1/2}\right]=0.43195$$

$$a^2=\Gamma\left(\frac{1}{4}\right)\Gamma\left(\frac{5}{4}\right)\Big/\Gamma^2\left(\frac{3}{4}\right)=2.1884$$

$$b=\frac{1}{2}\left\{3-\frac{\Gamma\left(\frac{1}{4}\right)\Gamma\left(\frac{5}{4}\right)}{\Gamma^2\left(\frac{3}{4}\right)}\right\}=0.40578$$

(2) Numerical Results and Discussion

With the aid of the results in the previous section, the probability density and the probability distribution of the maximum response in terms of the peak envelope have been computed from Eqs. (25) and (26) the result of which is shown in Fig. 11 whose abscissas are normalized with respect to σ_{ym}. Then the mean value $\mathrm{E}[Y]$ is obtained by a numerical integration as

$$\mathrm{E}[Y]\cong\int_0^{\infty} Y\phi_E(Y)dY=2.5038\sigma_{ym} \qquad \cdots\cdots\cdots\cdots(32)$$

To obtain the probability distribution of the maximum response from these results, we must determine σ_{ym}. It is not always reasonable to let σ_{ym} be equal to the maximum r.m.s. response $\sigma_{y\max}$ shown in Fig. 5, since $\sigma_{y\max}$ is only

* The interval of integration is extended to negative infinity. However, its effect on the result of integration is neglible as long as Eq. (29) is used.

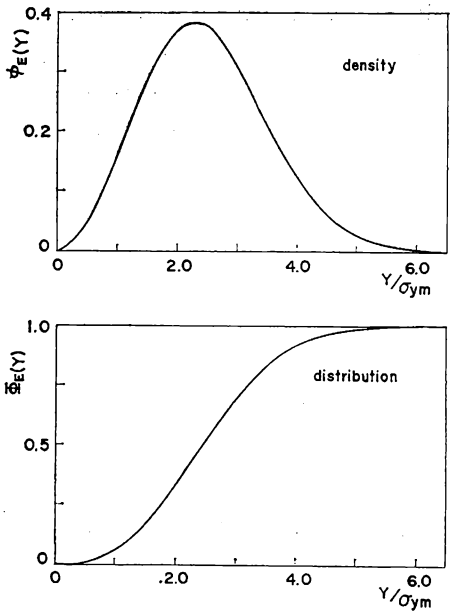

Fig. 11. Probability Density and Distribution of Peak Envelope.

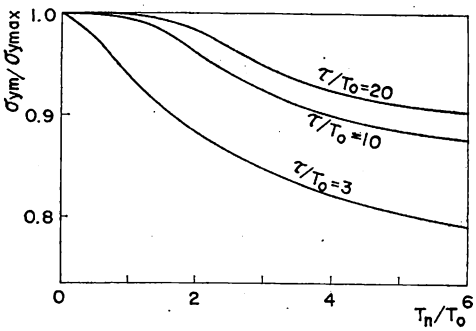

Fig. 12. Reduction Factor to Determine σ_{ym}.

the peak value and the average r.m.s. response in the time interval containing $\sigma_{y\max}$ is somewhat lower. Fig. 12 shows the reduction factor represented by the ratio of σ_{ym} to $\sigma_{y\max}$ which has been so determined as to give best agreement between analytical and simulated values of $\Phi(Y)$ for higher levels of of Y. Hence, by reference to Figs. 5 and 12, the average r.m.s. response σ_{ym} is determined, and on substituting it into Eqs. (25) and (26) or applying it to Fig. 11 we obtain the probability distribution of the maximum response in terms of the peak envelope distribution.

The peak envelope method adopted in this subsection is an approximate method, as was the pure-birth-process method, in obtaining the probability distribution of the maximum response. Hence, its accuracy has been examined in relation to the experimental values obtained from numerical simulation. Figs. 13~15 show some examples of the analytical and the simulated results for the same values of parameters as in Figs. 6~8. It is observed in these figures that the analytical and the simulated values are in better agreement for larger T_n/T_0 and smaller τ/T_0 in contrast to Figs. 6~8 showing the result of the pure-birth-process method. Since Eq. (25) derived from the peak envelope method has been obtained by neglecting the effect of the subsiding tail of $\sigma_y(t)$, the error caused by it becomes greater, as this subsiding tail has

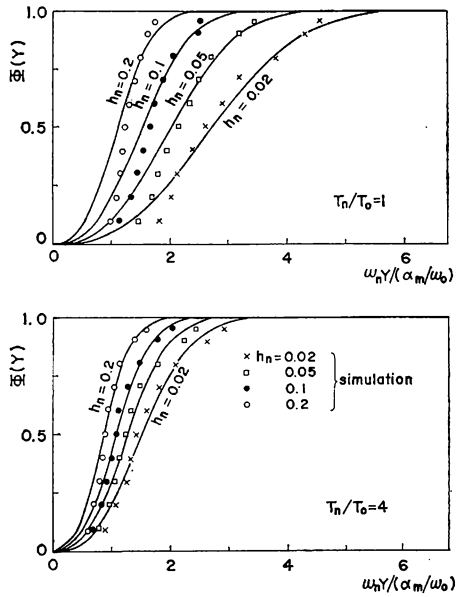

Fig. 13. Probability Distribution of the Maximum Earthquake Response Based on the Peak Envelope Method ($\tau/T_0=3$).

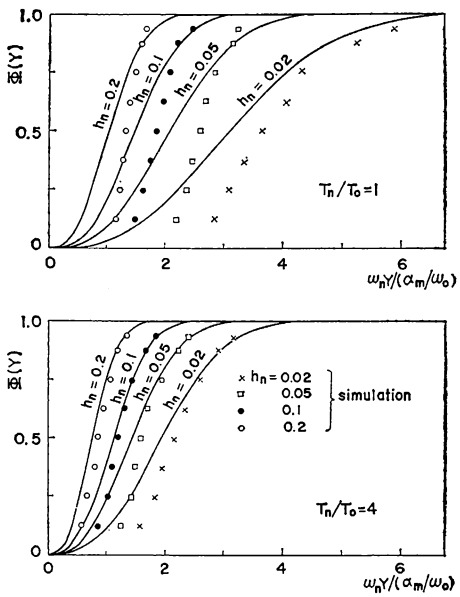

Fig. 14. Probability Distribution of the Maximum Earthquake Response Based on the Peak Envelope Method ($\tau/T_0=10$).

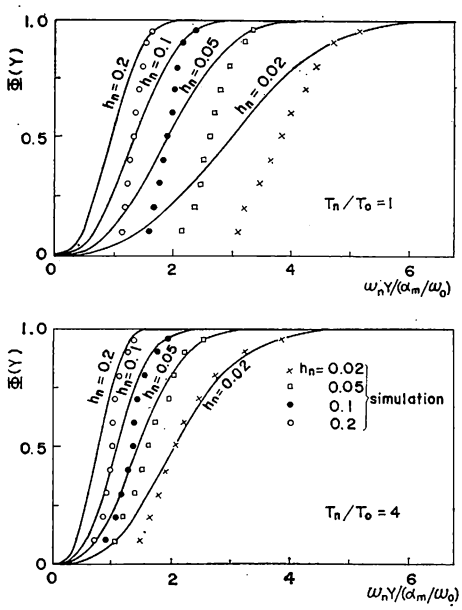

Fig. 15. Probability Distribution of the Maximum Earthquake Response Based on the Peak Envelope Method ($\tau/T_0=20$).

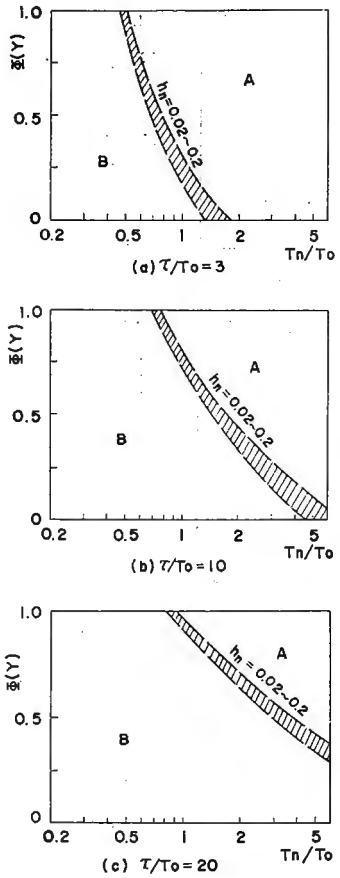

Fig. 16. Precision Zoning for the Peak Envelope Method.

enough of a random nature to contribute to the evaluation of the maximum response, which is the case where the pure-birth-process method is accurate. Fig. 16 shows the ranges of parameters denoted by the domain "A" in which the peak envelope method is applicable, and that, domain "B", in which it cause great approximation error. The domains "A" and "B" in this figure have been determined in the same sense as in Fig. 9. It is noted in Fig. 16 that the zoning of "A" and "B" domains has been made by a single hatched belt, accounting for the damping factor in the range h_n=0.02~0.2, since the numerical results show that the approximation error due to the peak envelope method does not depend greatly upon h_n, whereas the effect of h_n is great in the pure-birth-process method as we have seen in Fig. 9.

By comparing Fig. 9 and Fig. 16, or Figs. 6~8 and Figs. 13~15, it is noted

that the two methods of analysis of the probability distribution of the maximum earthquake response can be combined with each other to cover a wide range of the structural and the excitation parameters.

6. Probabilistic Parameters of the Maximum Earthquake Response Related to Structural Design Criteria

The foregoing discussions in this study have been devoted to the development of methods of analysis with which to obtain the probability distribution of the maximum earthquake response of simple structures, of which the pure-birth-process method and the peak envelope method have proved to give good approximations for certain ranges of parameters. If we use these methods alternatively, we can obtain the statistics of the maximum earthquake response for a wide range of parameter values, on the basis of which there can be deduced several probabilistic parameters relevant to structural design practice. As pointed out in **1**, the probability distribution $\Phi(Y)$ of the maximum response is in itself an important parameter directly connected with the reliability function of the structure. In design practice, however, it is desirable that these statistical data be represented in more compact forms to facilitate reference by engineers. For this purpose, this chapter presents the numerical values for the mean value and the relative dispersion of the maximum response represented in the form of response spectra, by which the over-all statistical characteristics of the maximum response can be discussed.

(1) Mean Response Spectra

By setting

$$S_D=\mathrm{E}[Y], \quad S_V=\omega_n S_D, \quad S_A=\omega_n^2 S_D \qquad \cdots\cdots\cdots\cdots(33)$$

and plotting them against the natural period of the structure, we obtain the mean response spectra of displacement, pseudo velocity, and acceleration, respectively. In this manner the concept of the average response spectra developed by G. W. Housner[11] was generalized to response statistics with a broader probabilistic background, or, conversely, the analyses developed in this chapter can be discussed in direct relation to the results of the response analysis for real earthquake records.

Thus Figs. 17 and 18 show the mean response spectra obtained by use of the pure-birth-process method and the peak envelope method, respectively, both plotted along with the experimental values due to the numerical simulation. The analytical values have been calculated from Eqs. (24) and (32). It is noted from these figures that the approximation error caused by the two

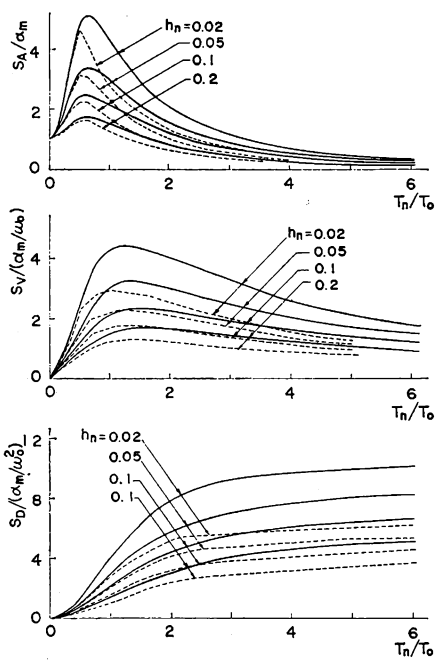

(a) $(\tau/T_0=3)$

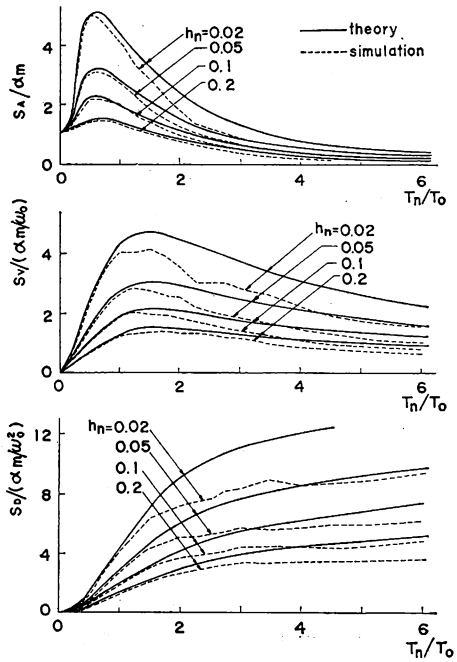

(b) $(\tau/T_0=10)$

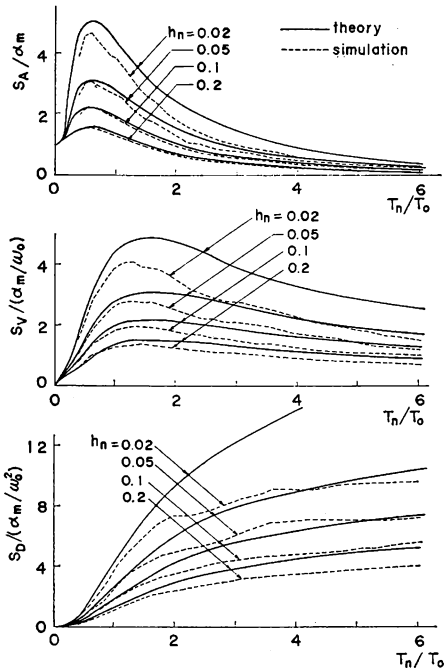

(c) $(\tau/T_0=20)$

Fig. 17 Mean Response Spectra Based on the Pure-Birth-Process Method.

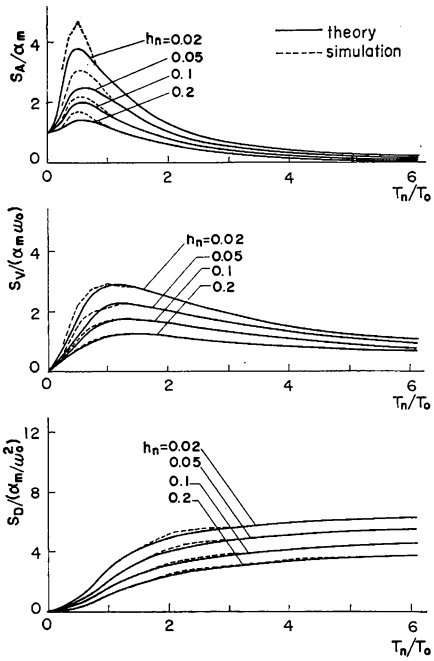

(a) $\tau/T_0=3$

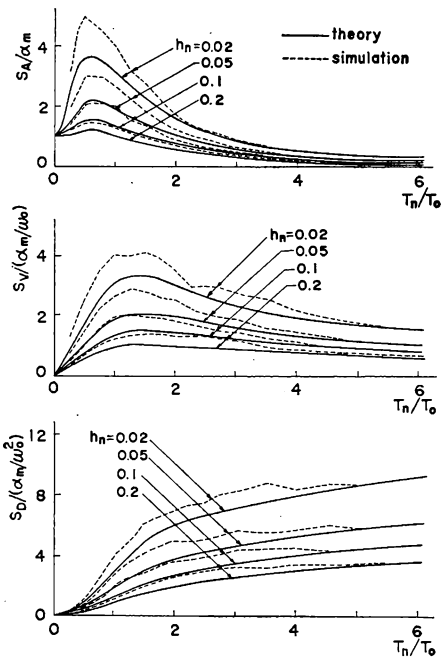

(b) $\tau/T_0=10$

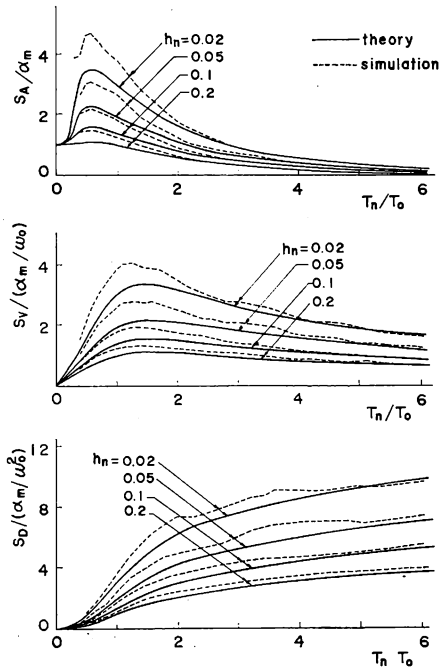

(c) $\tau/T=20$

Fig. 18. Mean Response Spectra Based on the Peak Envelope Method.

methods behaves in the same manner as discussed for $\Phi(Y)$ in the foregoing chapters; i.e., the pure-birth-process method is valid for relatively small T_n/T_0 and large τ/T_0 and h_n, and the peak envelope method, for large T_n/T_0 and small τ/T_0.

It is noted also that when the damping factor h_n is small the response becomes higher with increasing τ/T_0, which implies that for impulsive earthquakes of short duration the response does not grow large. This argument coincides with the result of the observation of real earthquakes.[5] Hence, in discussing the maximum response, the estimation of the duration of excitation plays an important role.

It is readily understood that the shape of these mean response spectra is affected by the parameter h_0 in Eq. (5) to determine the sharpness of the spectral density of excitation. The value $h_0=0.9$ used herein has been chosen so that the acceleration spectra might take on peak values somewhat close to those in the average response spectra for real earthquakes.[11,12] However, it should be kept in mind that those average response spectra for real earthquakes are based on various types of accelerograms which cannot be said to have been picked up from a single population. In this sense, the value $h_0=0.9$ is by no means to be fixed for all earthquakes, but it is to vary with various ruling parameters related to the site conditions and the intensity of the earthquakes. Including this problem, the analysis of earthquake motion supported by strong motion accelerograph networks is an important future task by which to establish reasonable models of earthquake motion.

(2) Relative Dispersion Spectra

Let C_v denote the relative dispersion of Y. Then C_v represents the standard deviation σ_Y of Y normalized with respect to its mean value; i.e.,

$$C_v=\frac{\sigma_Y}{S_D}=\frac{\{\mathrm{E}[Y^2]-(\mathrm{E}[Y])^2\}^{1/2}}{\mathrm{E}[Y]} \qquad \cdots\cdots(34)$$

Hence, for the evaluation of C_v, the mean square $\mathrm{E}[Y^2]$ must be obtained in advance. The mean square of Y according to the peak envelope method is obtained by numerical integration as

$$\mathrm{E}[Y^2]\cong\int_0^\infty Y^2\phi_E(Y)dY=7.3269\sigma^2_{ym} \qquad \cdots\cdots(35)$$

Since the pure-birth-process method provides only the distribution function $\Phi(Y)$, we shall use Eq. (A.4) of the Appendix valid for an arbitrary random variable. Since Y assumes only non-negative values, we have

$$\mathrm{E}[Y^2]=2\int_0^\infty dY\int_Y^\infty\{1-\Phi(Y')\}dY' \qquad \cdots\cdots(36)$$

The numerical results for C_v are shown in Fig. 19. It is remarkable that the numerical values for the pure-birth-process method (p.b.p.m.) are greatly smaller than those for the peak envelope method (p.e.m.). The p.e.m. value is equal to 0.41083 by virtue of Eqs. (32) and (34). The p.b.p.m. value varies slightly but takes on almost constant values regardless of parameter values considered herein. On the other hand, the simulated values, on the whole, vary between these two analytical values, in which it is natural, from the foregoin discussion of the approximation error, that the simulated results are close to the p.b.p.m. values for small T_n/T_0 and large τ/T_0 and to the p.e.m. values for large T_n/T_0 and small τ/T_0.

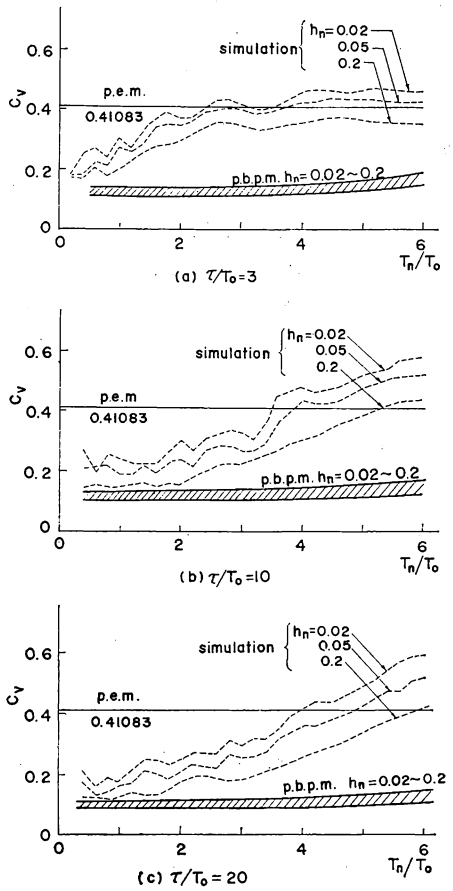

Fig. 19. Relative Dispersion Spectra of the Maximum Response (p.b.p.m. : pure-birth-process method, p.e.m. : peak envelope method; $C_v=\sigma_Y/S_D$).

Table 2. Maximum Response Relative to Its Mean Value for Various Non-Excess Probability Levels.

$\Phi(Y)$	$Y/E(Y)$	
	pure-birth-process method*	peak envelope method
0.98	1.287	1.927
0.95	1.216	1.725
0.9	1.157	1.548
0.8	1.092	1.350
0.7	1.051	1.198
0.6	1.017	1.078
0.5	0.9878	0.9705

* $h_n=0.05$, $T_n/T_0=1$, $\tau/T_0=10$. Similar results have been obtained for other cases.

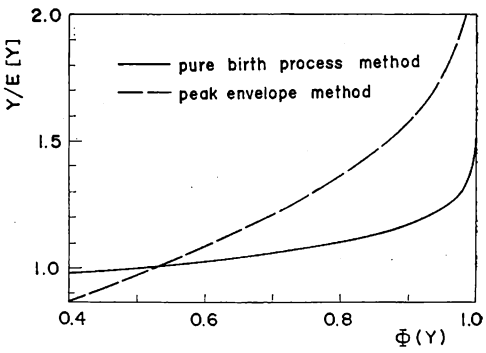

Fig. 20. Maximum Response Relative to Its Mean Value vs. the Non-Excess Probability.

From the viewpoint of structural design, it should be noted that due to the large value of C_v for large T_n/T_0, the maximum response of a structure with a relatively long natural period disperses in a wider range about its mean value than the case of a relatively short natural period. In other words, even if a structure is so designed as to have the strength of a constant value times the response level read off from a mean response spectrum, the non-excess probability of the response, or the probability of structural safety, varies with the natural period. Thus, under the requirement of an equal probability of structural safety, a higher level of the maximum response relative to its mean should be chosen as a design criterion for large T_n/T_0 than for small T_n/T_0.

For cases where either the pure-birth-process method or the peak envelope method is valid, the value of the maximum response corresponding to a given non-excess probability can be read off from Figs. 6~8 or Figs. 13~16, or when the discussion is made in terms of the ratio $Y/E[Y]$, from Table 2 and Fig. 20. The results of the pure-birth-process method in Table 2 and Fig. 20 are given only for $h_n=0.05$, $T_n/T_0=1$, and $\tau/T_0=10$. However, as long as the ratio of the maximum response to its mean value is under discussion, similar results have been obtained for other values of parameters. Thus, it could be stated, for example, that to ensure a 95 percent probability of structural safety, it suffices to adopt as design criteria 1.2 times the ordinate of the mean response spectra for structures with relatively short natural periods and 1.7 times for structures with longer natural periods.

7. Conclusions

This study has dealt with the probability distribution of the maximum response of linear structures subjected to random earthquake excitation, from which the following conclusions have been derived.

(1) In discussing the random earthquake motion, various types of non-stationarity in amplitude can be discussed in terms of the equivalent duration proposed in this study.

(2) There have been developed two methods of analysis of the maximum structural response to random earthquake excitation, which have been tentatively called the pure-birth-process method and the peak envelope method, respectively.

(3) From the error survey made with the aid of a numerical simulation, it can be said that the pure-birth-process method is applicable to a structure with a relatively short natural period subjected to an earthquake motion of a relatively long duration and the peak envelope method, to the case of a rel-

latively long natural period and an impulsive earthquake motion.

(4) The pure-birth-process method and the peak envelope method combine with each other to cover a wide range of structural and excitation parameters. To know which of the two methods should be adopted for a given set of parameters, Figs. 9 and 16 for precision zoning are available.

(5) For design purpose, it would be convenient to make use of data, represented in a compact form of the mean response spectra and the relative dispersion spectra, Figs. 17~19, and of the relation between the maximum response relative to its mean value and the specified non-excess probability, Table 2 and Fig. 20, by which the maximum response is discussed in terms of the mean value and dispersion about it.

(6) The relative dispersion of the maximum earthquake response varies with the natural period and the duration of the earthquake. For a specified probability of structural safety, a higher level of the maximum response relative to its mean value should be adopted as the design strength for structures with long natural periods than for those with short natural periods.

As pointed out in this chapter, it is in general difficult to obtain an exact solution for the probability of a structural event in a finite duration of random vibration. Hence, in most cases a theoretical treatment can only provide us with approximate results, for which the approximation error can be inspected with the aid of a numerical simulation, which has been the general procedure adopted in this study. It is noted that the numerical simulation itself can be a powerful tool of basic analysis, since it will offer results as close to the exact solution as we wish if a sufficiently large sample size is taken. However, analytical methods, even if approximate, are far superior to the numerical simulation in investigating the details of the phenomena and their physical significance, by which insight into the problem is greatly deepend. Hence, in the study of structural safety in earthquakes by means of the random vibration theory, it is desirable to make effective use of these two methods together.

Acknowledgment

The contents of this paper were presented in a chapter of the author's doctoral thesis[14] submitted to Kyoto University which was completed under the guidance of Professor Hisao Goto, to whom the author would like to express sincere appreciation for his invaluable advice and encouragement. The numerical computation in this study was made on the digital computer FACOM

230-60 of the Data Processing Center, Kyoto University.

References

1) Caughey, T. K., and Stumpf, H. J.; "Transient Response of a Dynamic System under Random Excitation", *Jour. Appl. Mech.*, Ser. E, No. 4, Dec., 1961, pp. 563-566.
2) Davenport, A. G.; "The Application of Statistical Concepts to the Wind Loading of Structures", *Proc. ICE*, Vol. 19, 1961, pp. 449-472.
3) Freudenthal, A. M., and Shinozuka, M.; "Probability of Structural Failure under Earthquake Acceleration", *Trans. JSCE*, No. 118, June, 1965, pp. 9-15.
4) Freudenthal, A. M., Garrelts, J. M., and Shinozuka, M.; "The Analysis of Structural Safety", *Proc. ASCE*, Vol. 92, ST 1, Feb., 1966, pp. 267-325.
5) Goto, H., Toki, K., Yokoyama, Y., Kameda, K., Akiyoshi, T., and Ishida, M.; "Seismic Observations in the Region of Matsushiro Earthquakes", *Trans. JSCE*, No. 145, Sep., 1967, pp. 1-11, (in Japanese).
6) Goto, H., and Kameda, H.; "A Statistical Study of the Maximum Ground Motion in Strong Earthquakes", *Mem. Fac. Engng., Kyoto Univ.*, Vol. XXIX, Part 4, Oct., 1967, pp. 389-419.
7) Goto, H., and Kameda, H.; "A Statistical Study of the Maximum Ground Motion in Strong Earthquakes", *Trans. JSCE*, No. 159, Nov., 1968, pp. 1-12, (in Japanese).
8) Goto, H., and Kameda, H.; "Statistical Inference of the Future Earthquake Ground Motion", *Proc. IV WCEE*, Vol. 1, 1969, pp. 39-54.
9) Goto, H., and Kameda, H.; "On the Probability Distribution of the Maximum Structural Response in Random Vibration", *Ann., Disaster Prevention Res. Inst., Kyoto Univ.*, No. 11A, March, 1968, pp. 239-253, (in Japanese).
10) Goto, H., and Kameda, H.; "On the Probability Distribution of the Maximum Structural Response in Random Vibration, —Transient Response to Stationary Input—" *Ann., Disaster Prevention Res. Inst., Kyoto Univ.*, No. 12A, March, 1969, pp. 289-299, (in Japanese).
11) Housner, G. W.; "Limit Design of Structures to Resist Earthquakes", *Proc. WCEE*, S. F., June, 1956, pp. 5·1-5·13.
12) JSCE, ed.; *Vibration Handbook for Civil Engineers*, 1966, (in Japanese).
13) Kameda, H.; "On the Probability Distribution of the Maximum Structural Response in Earthquakes and Mean Response Spectra", *Proc. 25th Ann. Conf. JSCE*, Vol. I, pp. 509-512, (in Japanese).
14) Kameda, H.; "Fundamental Studies on Probabilistic Methods of Structural Design to Resist Earthquakes", Doctoral Thesis submitted to Kyoto Univ., March, 1971.
15) Komatsu, S.; "Design Method and Safety of Long-Span Suspension Bridge Against Wind", *Trans., JSCE*, No. 142, June, 1967, pp. 10-19, (in Japanese).
16) Rice, S. O.; "Mathematical Analysis of Random Noise", *Selected Papers on Noise and Stochastic Processes*, N. Wax, ed., Dover, 1954, pp. 133-294.
17) Rosenblueth, E., and Bustamante, J. I.; "Distribution of Structural Response to Earthquakes", *Proc. ASCE*, Vol. 88, EM3, June, 1962, pp. 75-106.
18) Shinozuka, M., and Sato, Y.; "On the Numerical Simulation of Nonstationary Random Processes", *Tech. Rep., Inst. Fatigue and Reliability, Columbia Univ.*, No. 31, April, 1966, pp. 1-44.
19) Toki, K.; "Earthquake Response of Structure and Its Foundation", Doctoral Thesis submitted to Kyoto Univ., March, 1969, pp. 151-156, (in Japanese).
20) Yamada, Y. and Takemiya, H.; "Studies on the Statistical Aseismic Safety of Relatively Long Period Structures", *Proc. JSCE*, No. 172, Dec., 1969, pp. 63-78.

Appendix. Representation of the Mean Value and Higher Moments of a Random Variable in Terms of the Probability Distribution Function

The moment $\mathrm{E}[z^n]$ of degree n of a random variable z is defined as

$$\mathrm{E}[z^n]=\int_{-\infty}^{\infty} z^n\phi(z)dz \qquad \cdots\cdots\cdots\cdots(\mathrm{A}\cdot 1)$$

where $\phi(z)$ is the probability density function of z which is related to the probability distribution function $\Phi(z)$ in the form

$$\int_{-\infty}^{z}\phi(z)dz=\Phi(z) \qquad \cdots\cdots\cdots\cdots(\mathrm{A}\cdot 2)$$

It is often the case that only the distribution function $\Phi(z)$ is known to us either in an analytical or numerical expression. In such a case, Eq. (A·1) to give the moment $\mathrm{E}[z^n]$ fails to be available, and it may in general cause a great error to obtain $\phi(z)$ by numerical differentiation of Eq. (A·2). Hence, in what follows we shall derive a formula which gives $\mathrm{E}[z^n]$ in terms of integrals involving only the distribution function $\Phi(z)$.

First, we shall consider the mean value $\mathrm{E}[z]$. Let G be an arbitrary positive number. Then we have

$$\begin{aligned}\int_{-G}^{G} z\phi(z)dz&=[z\Phi(z)]_{-G}^{G}-\int_{-G}^{G}\Phi(z)dz\\&=\int_{0}^{G}\{\Phi(G)-\Phi(z)\}dz-\int_{-G}^{0}\{\Phi(z)-\Phi(-G)\}dz=D_1(G)\end{aligned}$$

Since $\Phi(\infty)=1$ and $\Phi(-\infty)=0$, we obtain

$$\mathrm{E}[z]=\lim_{G\to\infty} D_1(G)=\int_{0}^{\infty}\{1-\Phi(z)\}dz-\int_{0}^{\infty}\Phi(z)dz \qquad \cdots\cdots\cdots\cdots(\mathrm{A}\cdot 3)$$

The mean square $\mathrm{E}[z^2]$ is obtained in a similar manner; i.e., we have

$$\begin{aligned}\int_{-G}^{G} z^2\phi(z)dz&=[z^2\Phi(z)]_{-G}^{G}-2\left[z\int_{0}^{z}\Phi(z_2)dz_2\right]_{-G}^{G}+2\int_{-G}^{G}dz_1\int_{0}^{z_1}\Phi(z_2)dz_2\\&=2\left[\int_{0}^{G}dz_1\int_{z_1}^{G}\{\Phi(G)-\Phi(z_2)\}dz_2+\int_{-G}^{0}dz_1\int_{-G}^{z_1}\{\Phi(z_2)-\Phi(-G)\}dz_2\right]=D_2(G)\end{aligned}$$

Hence, $\mathrm{E}[z^2]$ is obtained as

$$\begin{aligned}\mathrm{E}[z^2]&=\lim_{G\to\infty} D_2(G)\\&=2\left[\int_{0}^{\infty}dz_1\int_{z_1}^{\infty}\{1-\Phi(z_2)\}dz_2+\int_{-\infty}^{0}dz_1\int_{-\infty}^{z_1}\Phi(z_2)dz_2\right] \qquad \cdots\cdots\cdots\cdots(\mathrm{A}\cdot 4)\end{aligned}$$

For the general case of the n-th moment $\mathrm{E}[z^n]$, the discussion can be made in the same manner by means of successive integration by parts and of the relation

$$G^k = k!\int_0^G dz_1 \int_{z_1}^G dz_2 \cdots\cdots \int_{z_{k-1}}^G dz_k$$

Thus we obtain the following general formula:

$$\begin{aligned} \mathrm{E}[z^n] = n!\Big[& \int_0^\infty dz_1 \int_{z_1}^\infty dz_2 \cdots\cdots \int_{z_{n-1}}^\infty \{1-\Phi(z_n)\}dz_n \\ & + (-1)^n \int_{-\infty}^0 dz_1 \int_{-\infty}^{z_1} dz_2 \cdots\cdots \int_{-\infty}^{z_{n-1}} \Phi(z_n) dz_n \Big] \end{aligned} \qquad \cdots\cdots\cdots\cdots (\mathrm{A}\cdot 5)$$